# Naval Surface Warfare Center, Carderock Division

Bethesda, MD 20817-5700

NSWCCD-50-TR-1999/015  April 1999

Hydromechanics Directorate
Research and Development Report

# VMP WATERJET TEST RESULTS

by

John F. McMahon

Roderick W. Burke

Charles M. Dai

James W. Hickok

John G. Hoyt III

NSWCCD-50-TR-1999/015  April 1999 VMP WATERJET TEST RESULTS

19990430 017

DTIC QUALITY INSPECTED 4

Carderock Division, Naval Surface Warfare Center
Bethesda, MD 20817-5700

# VMP WATERJET TEST RESULTS

by

John F. McMahon

Roderick W. Burke

Charles M. Dai

James W. Hickok

John G. Hoyt III

(THIS PAGE INTENTIONALLY LEFT BLANK)

# CONTENTS

# FIGURES

# TABLES

# NOMENCLATURE

a,b,c – Coefficients in Exponential Curve for Capture Area Velocity Profiles

$A$ – Area $(ft^2)$

$A_w$ – Wetted Area – $(ft^2)$

$c_H$ – Head Coefficient - $2gH/V_S^2$

$c_m$ – Flow Coefficient - $Q/(V_S A_w)$

$c_{p\text{-}static}$ – Static Pressure Coefficient – $(p-p_o)/(1/2\rho V_S^2)$

$c_{p\text{-}total}$ – Total Pressure Coefficient – $[(p-p_o)/\rho+V^2/2]/(1/2V_S^2)$

$c_{pmin}$ – Blade Minimum Pressure Coefficient at Tip – $(p_{min}-p_I)/1/2\rho w^2$

$c_q$ – Volume Flow Coefficient for Reynolds' Number Correction– $Q/(V_S l w_0)$

$D$ – Ship Resistance – (lb)

$H$ – Pump Head – (ft)

$HP_{fluid}$ – Fluid Horsepower

IVR – Inlet Velocity Ratio – $(V_{mass})_{INLET}/(V_{mass})_{CAPTURE}$

$h$ – Depth Required for Cavitation Free Operation – (ft)

$k$– Passage Loss Coefficient

$l$ – Length from Front of Ship to Propulsor Inlet – (ft)

$m$ – Mass Flow Rate – (slugs/sec)

$p$ – Local Static Pressure – $(lb/ft^2)$

$p_o$ – Reference Static Pressure (Atmospheric) – $(lb/ft^2)$

$p_{min}$ – Minimum Blade Surface Static Pressure At Tip Section – $(lb/ft^2)$

$p_I$ – Static Pressure At Inlet Station – $(lb/ft^2)$

$Q$ – Volume Flow Rate – $(ft^3/sec)$

$V$ – Local Velocity – (ft/sec)

$V_D$ – Duct Velocity – (ft/sec)

$V_S$ – Ship Speed – (ft/sec or knots)

$V_{mass}$ – Flow Rate Averaged Velocity – (ft/sec)

$V_{mom}$ – Momentum Averaged Velocity – (ft/sec)

$V_{energy}$ – Energy Averaged Velocity – (ft/sec)

$w$ – Inlet Velocity Relative To the Blade At the Tip – (ft/sec)

$w_o$ – Average Width of Capture Area – (ft)

$(Re)_F$ – Length Reynolds' Number at Full Scale – $V_S l/\nu$

$(Re)_M$ – Length Reynolds' Number at Model Scale – $V_Sl/\nu$

$T$ – Propulsor Thrust – (lb)

$t$ – Hull Interaction Effect – $1-D/T$

$SHP$ – Shaft Horsepower

$\delta$ - Boundary Layer Thickness – (ft)

$\eta_P$ – Pump Efficiency – $HP_{fluid}/SHP$

$\eta_H$ – Hydraulic Efficiency

$\eta_I$ – Ideal Efficiency

$\eta_{inlet}$ – Inlet Efficiency – $[(V_{energy})_{INLET}/(V_{energy})_{CAPTURE}]^2$

$\nu$ - Kinematic Viscosity – $(ft^2/sec)$

$\rho$ - Fluid Density – $(lb\ sec^2/ft^4)$

# ABSTRACT

*This report presents the results of a series of waterjet experiments using twin, nearly vertical inlets and a nozzle with an underwater discharge conducted on a 1:24.8 scale model of a DDG 51 hull. The aft end of the hull was redesigned considerably both to accommodate the waterjet and to take advantage of potential propulsor/hull interactions.*

*This is a unique application. The DDG 51 parent hull is a displacement hull operating at speeds lower than what is typical for waterjets. In addition, the aft portion of the hull, the waterjet inlet, and the nozzle were executed as an integrated design to investigate taking advantage of both boundary layer and afterbody flows.*

*Total pressure, static pressure and velocities are presented at three measuring stations, one along the hull a short distance upstream of the waterjet inlet, the second inside of the inlet and the third in the jet a short distance downstream of the nozzle discharge. Surface pressure measurements along the hull, both upstream and downstream of the inlet, and within the duct are also presented.*

*A powering analysis of the results compared with a propeller driven hull indicated that the power requirement of the waterjet equipped hull was comparable and on the low side.*

# ADMINISTRATIVE INFORMATION

1

# SUMMARY

A series of waterjet self-propulsion tests were conducted in January of 1997 using a previously existing DDG51 model designated as 5482 but with a modified stern. The unit used two nearly vertical type of inlets and two underwater discharge jets characteristic of the Vertical
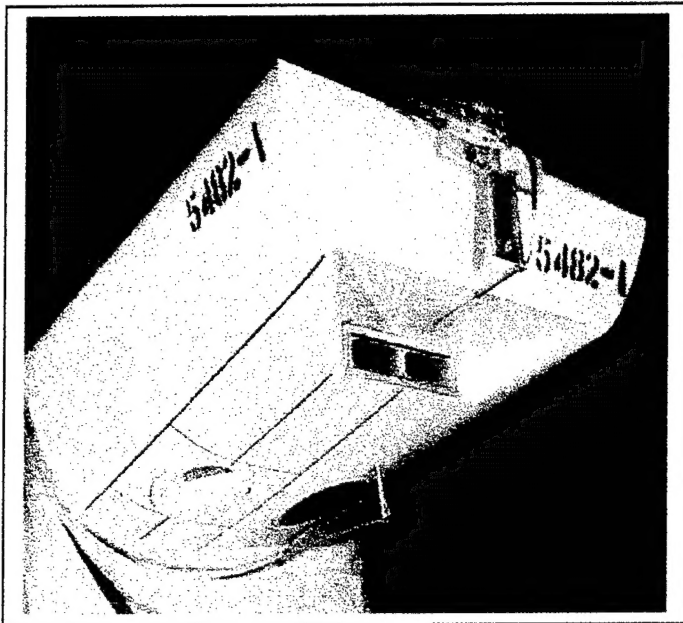
INTEGRATED VERTICAL INLET
PROPULSOR/HULL
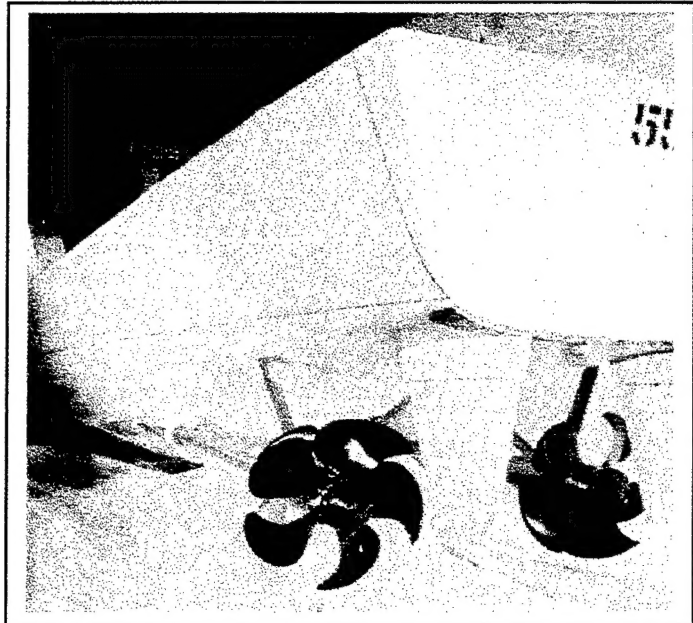
DDG-51 PROPULSION SYSTEM

**FIG. 1**
**VMP And Open Propeller Comparison**

Motor Propulsor (VMP) as described in Ref. 1. The inlet and jet areas were sized, based on a preliminary design analysis, for operation at a full-scale speed of 28 knots. The inlets and the stern modifications were designed by Dai [Ref. 1] as a fully integrated propulsor/hull design using the best computer tools that were available at the time. The major emphasis was on taking full advantage of the well-established, favorable propulsor/hull interaction associated with waterjets with respect to both the form drag and the wave drag of the hull form. For the purpose of model propulsion testing the two inlets were piped to a single, generic pump and the discharge of the pump was split and connected to the two jets. Fig. 1 shows both the modified 5482 hull and

a typical DDG51 hull equipped with a standard set of propellers. Data were taken at three speeds corresponding to full-scale speeds of 12, 20, and 28 knots based on Froude Number scaling. Self-propulsion data were taken at a resistance corresponding to the full-scale operation of the ship. This report covers the analysis of the data obtained in these experiments.

. The application is somewhat unique in several respects. One is that the DDG 51 is a displacement hull that operates at speeds somewhat lower than those characteristic of hulls with more conventional waterjet applications; another is the near vertical orientation of the inlet along with the underwater discharge and a third is the integrated design of the aft end of the hull and the waterjet inlet.
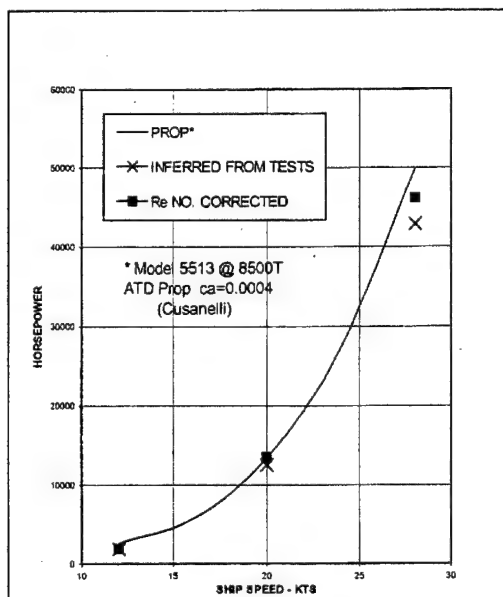


**FIG. 2**
**VMP/PROPELLER COMPARISONS**

The primary results are shown in Fig. 2 as a plot of the required horsepower versus ship speed. The solid line is the best available estimate for a comparable, propeller driven ship. The points labeled INFERRED FROM TESTS are full-scale projected results but without any correction for the Reynolds' Number effect on the hull boundary layer. The uncertainty in these results arising from the data collection and analysis is +/- 5%. The points labeled Re NO. CORRECTED contain a flat plate based correction for the hull Reynolds' Number effects; the uncertainty in this correction is unknown but relatively high. A pump efficiency of 85% at 28 knots was used.

A waterjet is a boundary layer inlet device and its performance is greatly affected by the boundary layer thickness. Assuming a zero pressure gradient along the bottom of the hull the height of the ingested layer at model scale was calculated to be in the neighborhood of 50% of the undisturbed boundary layer thickness. This is consistent with the test data that were obtained in the unpropelled condition. With the same zero pressure gradient assumption the height of the ingested layer at full scale was calculated to be larger than the boundary layer thickness. Consequently, the performance at full scale is probably considerably different than at model scale and so simplified corrections are quite questionable. Nevertheless, the results shown in Fig. 2

3

indicate that the waterjet would require no more horsepower than the propeller driven ship over the entire speed range and may use considerably less at some speeds.

As previously stated, the aft end of the model was modified not only to physically accommodate the waterjets but also to take advantage of the favorable propulsor/hull interaction. At an equivalent full-scale speed of 28 knots the thrust required to propel the modified hull was 13% less than the measured resistance of that hull at the same speed. Since this was the first effort at an integrated propulsor/hull design, achieving a favorable 13% propulsor/hull interaction is very encouraging. One would expect that with the rapid advance in design tools over the past few years even better results are possible.

No cavitation data were taken in these experiments. However, pressure measurements taken inside of the inlet indicate that the inlet itself would be cavitation free well in excess of 30 knots. It is estimated that the blade surfaces would be free of cavitation up to ship speeds in the neighborhood of 24 to 25 knots. However, waterjet inlets can be designed, at least conceptually, to achieve any desired cavitation performance. The inlet area of the current unit is relatively small as compared to most waterjets. A typical inlet area would be 30% larger than the current area and would raise the blade surface cavitation free speed from 24/25 knots to 28 knots even at the current submergence. Static pressure measurements taken along the hull and in the inlet indicate that the flow deceleration associated with the 30% increase in area could be obtained without flow separation in the inlet.

## MODELS

The afterbody of a hull model designated as Model 5482, an early variant of the DDG-51 hull form, was modified to accommodate the inlets and nozzles for two vertical motor propulsors (VMP) and re-designated as Model 5482-1. The hull was modified from mid-ship aft to integrate two elliptical inlets and two underwater discharging rectangular nozzles. The inlets, nozzles and the stern shape were designed by Dai [Ref. 1] as an integrated design, using the best computer tools available at the time, to take full advantage of the well established favorable propulsor/hull interactions with respect to both form and stern wave drag. For the purposes of model propulsion testing both inlets fed a common, generic pump whose exhaust was ducted into separate nozzles. The particulars for Model 5482-1 and the DDG-51 are given in Table 1.

4

## COMPARATIVE DATA

These results have been compared to the performance of the propeller driven DDG-51 using a variety of both model and full-scale results. A summary of the DDG-51 models known at the present time is included in Table 2.

| Particulars | Model Scale | Full Scale | DDG-51 |
|---|---|---|---|
| Scale Ratio | 24.824 | - | - |
| Waterline Length | 18.77 ft | 465.95 ft | 466.97 ft |
| Maximum Beam | | | 59.24 ft |
| Displacement | 1212 lbs FW | 8,500 lt SW | 8,740 lt SW |
| Surface Area | 51.96 ft$^2$ | 32,020 ft$^2$ | 32414 ft$^2$ |
| Duct Area per Jet | 9.62 in$^2$ | 41.17 ft$^2$ | - |
| Nozzle Area per Jet | 5.87 in$^2$ | 25.12 ft$^2$ | - |

### TABLE 1

### Model 5482-1 Particulars

| Model Number | Scale Ratio | Notes |
|---|---|---|
| 5415 | 24.824 | model hull identical to 5482, resistance data used for comparison to propeller variant |
| 5422 | 20.261 | no data available |
| 5482 | 24.824 | original model, no resistance data available, resistance data from model 5415 used |
| 5482-1 | 24.824 | modified model used in study |
| 5488 | 12.866 | no data available |
| 5513 | 20.261 | Used by Cusanelli & Karafiath in correlation study |

### TABLE 2

### Known Nominal DDG-51 Models

5

Since the original Model 5482 was never used for either resistance or self-propulsion experiments, the resistance data from Model 5415, which had the same scale ratio and hull form as Model 5482, were used for resistance comparisons. The raw model data, faired model data and expanded results for Model 5415 are given in Tables I-1, I-2, and I-3 of Appendix I. These results were measured with the model in the bare hull condition, which is with no keels, struts, shafts, or rudders. The expanded results use a correlation allowance of 0.0004 and an assumed overall propulsive coefficient of 0.66.
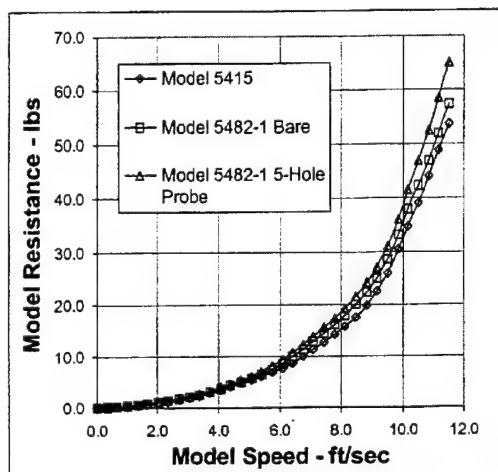


**FIG. 3**
**Comparison of Model Resistances**

Cusanelli and Karafiath, in a private communication included as Appendix II, provided the detailed powering performance of the DDG 51 that would give a realistic comparison for the results of these tests. They used the test results from Model 5513, which "includes several modifications --- to insure that the model is as closely representative of the full scale --- DDG 51 --- hullform as possible", adjusted to match the current test conditions.

**BARE HULL RESULTS**

The bare hull resistance of model 5482-1 was measured with the two elliptical inlet openings covered and faired into the hull. This model had no external shafts, struts, rudders or bilge keel. A waterjet variant would not have the shafts, struts or rudders but it would have the bilge keel. Resistance was measured with and without the 5-hole velocity probe used for the inlet survey in place. The raw and faired data measured for these two cases are given in Appendix III as Tables III-1 to III-4. Table 3 shows a comparison of the bilge keel drag and the difference between the model 5482-1 drag with and without the 5-hole velocity probe in place; it shows that added resistance due to the 5-hole probe is about the same as the bilge keel resistance. The powering data that will be described later were obtained using the 5-hole probe to simulate the bilge keel resistance. The resistance comparison between the 5482-1 bare hull, the 5482-1 hull with the 5-hole probe mounted and the parent, model 5415, is given in Fig. 3.

| Model Speed – ft/sec | Bilge Keel Drag Coef. | Bilge Keel Drag – lbs | 5Hole Probe Diff.-lbs | Re Correction – lbs |
|---|---|---|---|---|
| 2.71 | .00893 | 0.161 | 0.150 | 0.657 |
| 4.065 | .00872 | 0.377 | 0.309 | 1.343 |
| 5.420 | .00979 | 0.752 | 0.504 | 2.236 |
| 6.775 | .0114 | 1.374 | 0.912 | 3.323 |
| 8.130 | .0136 | 2.353 | 1.349 | 4.596 |
| 9.485 | .0163 | 3.829 | 2.487 | 6.048 |
| 10.840 | .0194 | 5.966 | 5.596 | 7.675 |

**TABLE 3**

**Comparison between Bilge Keel and 5-Hole Velocity Probe Resistance**

The last column in Table 3 is the increment that was subtracted from the model scale resistance to account for the model scale to full scale change in Reynolds' Number. This was determined by adjusting the skin friction part of the model resistance to account for the Reynolds' Number difference. It does not account for the Reynolds' Number effect on the hull boundary layer thickness at the capture area.

## METHODOLOGY

Fig. 4 is a sketch showing the stations at which data were obtained. The inlet and jet areas and the pitot/static rakes are shown to scale. The capture area was located at some distance upstream of the inlet. Data were taken at the capture area using a single tube, traversing pitot/static tube. The tube was pivoted so as to obtain data at the center of the inlet and at three transverse stations on each side of the center. A pitot/static rake was used within the inlet area and data obtained at the center and three additional radial stations. This rake was rotated and data taken at every $10^0$. A single pitot tube traversing in both
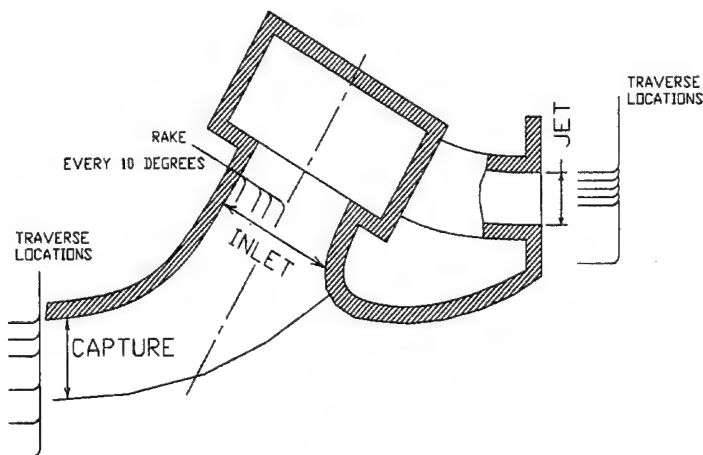


**FIG. 4**
**Measurement Stations**

the vertical and transverse direction was used to obtain data in the jet. Data were obtained at six vertical and five transverse locations.

A first principle based on Newton's Second Law with no other assumptions is that the rate at which energy is added to a ducted flow is the difference between the rate at which energy is being carried away and the rate at which it is being carried into the unit plus all of the energy losses in between. In equation form

$$\eta_p SHP = HP_{fluid} = \int_{JET} (\frac{p - p_o}{\rho} + \frac{V^2}{2})dm - \int_{INLET} (\frac{p - p_o}{\rho} + \frac{V^2}{2})dm + losses$$

where the station marked JET is any station downstream of the pump and the station marked INLET is any station upstream of the pump. The losses have to include all of the frictional losses between the two stations exclusive of the pump losses, which are covered by the $\eta_P$ on the left-hand side of the equation. Data sufficient to evaluate the two integrals were obtained in the tow tank experiments at self-propulsion conditions simulating full scale. The shaft horsepower required for any candidate propulsor can then be obtained by using these results along with a loss term that adequately describes the passage geometry of the candidate propulsor and a pump efficiency corresponding to the candidate pump.

For the tests reported here, there was only one measuring station downstream of the pump so there is no choice as to what location to use for the first integration. However, there were two upstream stations and so there is a choice as to which one to use. In the analysis that follows, the station marked as INLET in Fig. 4 was used. The primary reason for this was that it already includes the effect of the inlet loss, which is the major contributor to the losses. The loss term is empirical and so subject to question; therefore the less the loss term has to include the more reliable are the results. A second reason, as will be discussed later, is that integration at the capture area is very uncertain because of the uncertainty as to where the boundary of the ingested layer is located.

The results of the integrations in the above equation, as well as flow rate and momentum integrations will be presented as average velocities defined as follows:

8

$$V_{mass} = \frac{1}{A} \int dQ$$

$$V_{mom} = \frac{1}{\rho Q} \int [(p - p_o) + \rho V^2] dA$$

$$\frac{V_{energy}^2}{2} = \frac{1}{Q} \int [\frac{(p - p_o)}{\rho} + \frac{V^2}{2}] dQ$$

The static pressure term included in the momentum average was included at both the inlet and jet areas but not at the capture area. Using these average velocities, the first equation can be written as

$$\eta_P SHP = HP_{fluid} = \rho Q \frac{V_S^2}{2} [(\frac{V_{energy}}{V_S})^2_{JET} - (\frac{V_{energy}}{V_S})^2_{INLET} + k(\frac{V_D}{V_S})^2]$$

where $V_D$ is some suitably defined velocity in the duct and k is a loss coefficient associated with that velocity. In the current analysis either the inlet area can be used for the station marked INLET, in which case the inlet losses do not have to be included in the loss term, or the capture area can be used, in which case the inlet losses do have to be included in the loss term. The result would be the same in either case.

The method of analysis just described is identical to the ITTC [Ref. 2] recommended method of analysis with the exception that the inlet area rather than the capture area has been used for the upstream station. The ITTC recommendations use the capture area because data at the inlet area is difficult, if not impossible, to obtain for conventional, horizontal shaft units. One advantage of this method of analysis is that it does not have to deal with the propulsor/hull interaction. An additional advantage of using the inlet area for the upstream station is that the inlet loss is inherently included in the data.

9

The energy equation can be cast in another form by multiplying and dividing it by appropriate quantities. Thus

$$\eta_P SHP = \{\frac{\rho Q[\frac{V^2_{energyJET}}{2} - \frac{V^2_{energyINLET}}{2} + k(\frac{V_D}{V_S})^2]}{\rho Q[\frac{V^2_{energyJET}}{2} - \frac{V^2_{energyINLET}}{2}]}\} \{\frac{\rho Q[\frac{V^2_{energyJET}}{2} - \frac{V^2_{energyINLET}}{2}]}{TV_S}\} \{\frac{TV_S}{DV_S}\} DV_S$$

The first of these terms is the inverse of a hydraulic efficiency, the second is the inverse of the ideal propulsive efficiency, the third is the inverse of the propulsor/hull interaction and the last is the effective horsepower. This equation can then be rewritten as

$$SHP = \frac{HP_{eff}}{\eta_P \eta_H \eta_I (1-t)}$$

All of the data necessary to calculate these efficiencies and the propulsor/hull interaction were obtained in these tests and they will be presented later.

Both the ideal efficiency and the (1-t) term contain the propulsor thrust, a term that can be defined a number of different ways and is a subject of considerable debate. In this case it will be defined, as is, more or less, customary, as the momentum difference between the jet area and the capture area. That is

$$T = \rho Q[(V_{mom})_{JET} - (V_{mom})_{CAPTURE}]$$

Data at the capture area were obtained for both the self-propelled and the unpropelled case. For the unpropelled case the inlet and jet areas were blocked. There is a debate within the waterjet community as to whether the propelled or unpropelled data should be used; the propelled data was used in this analysis. In either case the three dimensionality of the flow makes analysis of the capture area data difficult, if not impossible. However, the propelled data at least led to consistent results; the unpropelled data did not.

# DATA ANALYSIS

Data were taken at models speeds of 4.094, 6.785 and 9.475 ft/sec which correspond to Froude Number scaled ship speeds of 12, 20 and 28 knots. All the pressures are shown as coefficients, that is

$$c_{p-static} = \frac{p - p_o}{\frac{1}{2}\rho V_S^2} \qquad c_{p-total} = \frac{(p - p_o) + \frac{1}{2}\rho V^2}{\frac{1}{2}\rho V_S^2}$$

where the reference pressure, $p_o$, is atmospheric pressure.

## FLOW RATES

Flow rates were obtained from measurements at the inlet area with the pump operating at the self-propulsion RPM. Since the drag coefficient of the ship increases with ship speed so should the non-dimensional mass flow rate defined as

$$c_m = \frac{m}{\rho V_S A_w}$$

This is borne out by the data shown in Table 4. This is in contrast to planning craft where the non-dimensional flow rate decreases as the ship speed increases.

| Full Scale Ship Speed Kts | Model Speed Ft/Sec | Model Flow Rate Ft$^3$/Sec | Mass Flow Coefficient $C_m$ |
|---|---|---|---|
| 12 | 4.094 | .228 | $1.079 \times 10^{-3}$ |
| 20 | 6.785 | .416 | $1.182 \times 10^{-3}$ |
| 28 | 9.475 | .625 | $1.268 \times 10^{-3}$ |

**TABLE 4**

**Flow Rates**

## INLET VELOCITIES

Data were obtained using a pitot/static rake at four radial locations and thirty six circumferential positions. The total and static pressure measurements obtained at a full-scale speed of 28 knots are shown in Fig. 5 and the resulting velocities in Fig. 6. The circumferential zero is along the centerline and on the downstream surface of the inlet. The data at 12 and 20 knots are very similar. Integration for the average velocities in the inlet area is straightforward. The results are shown in Table 5; the momentum average is not included because there is no need for it at this location.

| Full Scale Ship Speed | $V_{mass}/V_S$ | $V_{energy}/V_S$ |
|---|---|---|
| 12 | .847 | .714 |
| 20 | .904 | .789 |
| 28 | 1.012 | .826 |

**TABLE 5**
**Inlet Station Velocities**
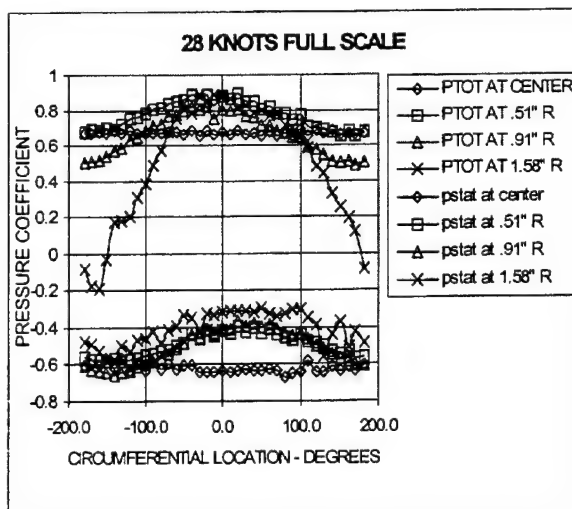


**FIG. 5**
**Total & Static Pressures At Inlet Area**
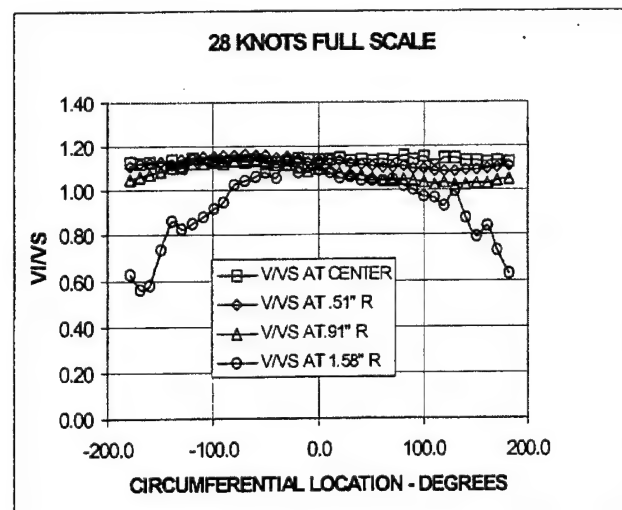


**FIG. 6**
**Velocities At Inlet Area**

## JET VELOCITIES

Data were obtained at five transverse stations and six vertical stations one of which was well outside of the jet as shown in Fig. 4. The static and total pressures at 28 knots are shown in

Fig. 7 and the velocities in Fig. 8. The jet velocities were measured at a station slightly downstream of the nozzle exit.

The edges of the jet are not very well defined. The integrations were performed by fixing both sides and the top of the jet and letting the bottom vary so as to obtain the mass flow rate
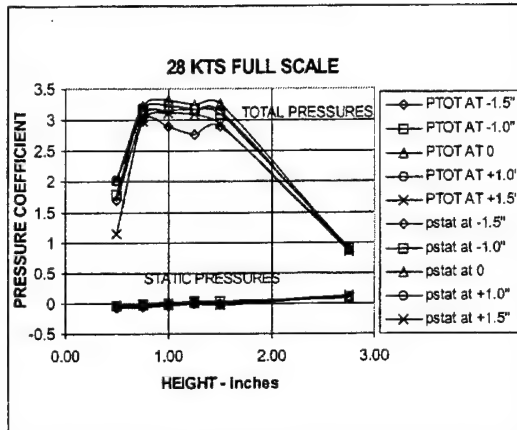


**FIG. 7**
**Jet Total & Static Pressures**
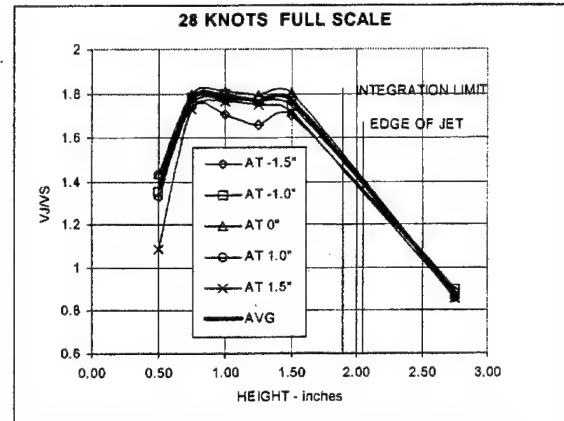


**FIG. 8**
**Jet Velocities**

measured at the inlet area. Since the jet velocity is the dominating term in the powering analysis the integrations were done not only at the measured mass flow rate but also 95% and 105% of the measured flow rate. This was an attempt to evaluate the uncertainty of the analysis. The results are shown in Table 6. The jet velocities all increase as the ship speed increases, as they should because of the increasing drag coefficient. The momentum averaged velocities are higher than the mass flow rate averaged velocities, as expected, but also higher than the energy averaged velocities, which was not expected. This arose because of the interpolation of the static pressure between the point at a height of 1.5 inches (well inside of the jet) and the point at a height of 2.75 inches (well outside of the jet). The momentum velocities are probably not correct, but they are used in the powering analysis. The variation in the energy averaged velocities between + and - 5% of the measured flow rate is less than 2%.

| SPEED | 95% FLOW RATE | | | MEASURED FLOW RATE | | | 105% FLOW RATE | | |
|---|---|---|---|---|---|---|---|---|---|
| KTS | $V_{mass}/V_S$ | $V_{mom}/V_S$ | $V_{energy}/V_S$ | $V_{mass}/V_S$ | $V_{mom}/V_S$ | $V_{energy}/V_S$ | $V_{mass}/V_S$ | $V_{mom}/V_S$ | $V_{energy}/V_S$ |
| 12 | 1.221 | 1.587 | 1.396 | 1.213 | 1.636 | 1.387 | 1.203 | 1.692 | 1.376 |
| 20 | 1.472 | 1.662 | 1.604 | 1.467 | 1.682 | 1.594 | 1.459 | 1.708 | 1.583 |
| 28 | 1.667 | 1.840 | 1.781 | 1.660 | 1.878 | 1.773 | 1.650 | 1.925 | 1.762 |

**TABLE 6**

**Jet Velocities**

## CAPTURE AREA VELOCITIES

There is some controversy within the waterjet community as to how to handle the capture area. Some investigators use the velocities measured along the centerline of the inlet at the unpropelled condition. As will be seen shortly, this procedure did not produce consistent results. However, the velocities measured along the centerline of the inlet under self-propelled conditions did produce consistent results.
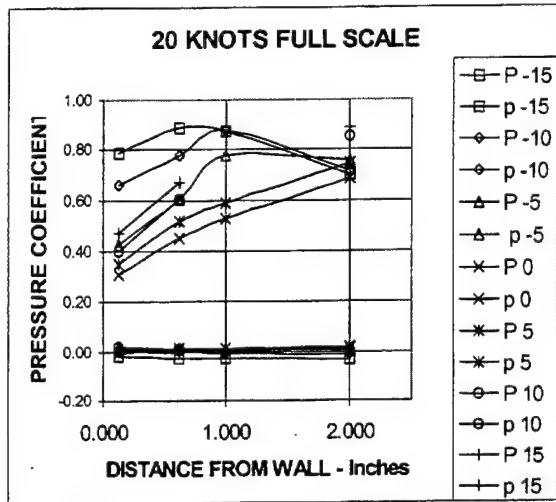


**FIG. 9**
**Unpropelled Capture Area Total & Static Pressures**
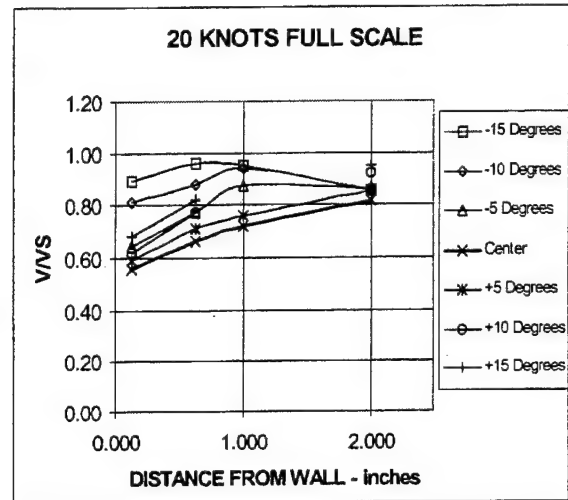


**FIG. 10**
**Unpropelled Capture Area Velocities**

The total and static pressures at the capture area with the inlet and exit blocked and the body towed (the unpropelled condition) are shown in Fig. 9 and the resulting velocities in Fig. 10. Fig. 9 shows that the static pressure is uniform across the flow, as would be expected for a flow where the streamlines have little or no curvature. Data are shown at a full-scale ship speed of 20 knots; the data at the other ship speeds were very similar. The considerable variation of total pressure and, consequently, velocity with transverse location is surprising and unexplained. The centerline velocity being the lowest of all is also surprising and is unexplained.

| SPEED | $V_{mass}/V_S$ | $V_{mom}/V_S$ | $V_{energy}/V_S$ |
|-------|---------------|---------------|------------------|
| 12 | .671 | .700 | .713 |
| 20 | .677 | .705 | .719 |
| 28 | .681 | .709 | .723 |

**TABLE 7**

**Unpropelled Capture Area Velocities**

14

Table 7 shows the velocities obtained at the capture area at the unpropelled condition. These velocities were obtained by curve fitting the centerline velocity with an exponential of the type

$$\frac{V}{V_S} = [1 - EXP(-a\frac{x}{b})]^{\frac{1+x}{c}}$$

and using this at all of the transverse locations. Because of the additional complexities in curve fitting the static pressure, it was not included in either the momentum or energy averages. The capture area was assumed to be elliptical with the ellipse sized so as to capture the correct mass flow. These velocities are surprisingly low; in fact the energy-averaged velocities are less than those obtained in the inlet area (see Table 6), a clearly impossible condition. Even using higher
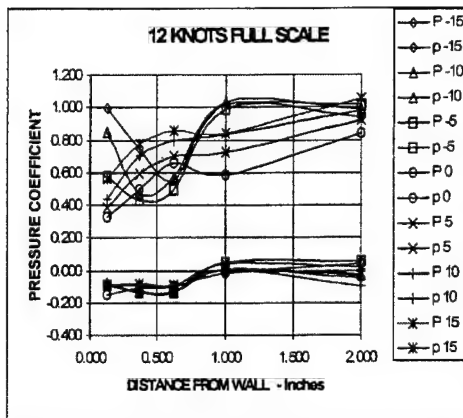


**FIG. 11**
**Self-Propelled Capture Area Total &**
**Static Pressures**
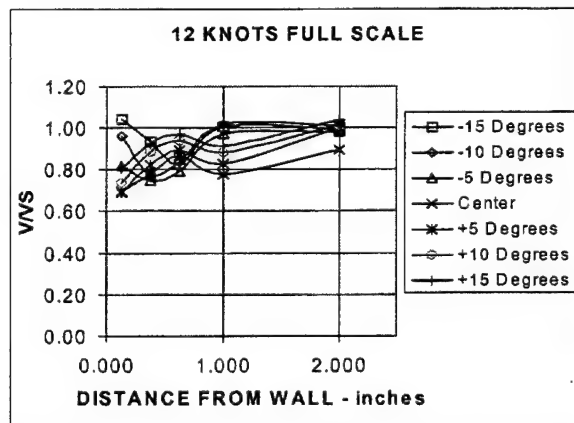
**FIG. 12**
**Self-Propelled Capture Area Velocities**

velocities measured in the off-centerline locations would not improve the situation very much.

The total and static pressures at 12 knots under self-propelled conditions are shown in Fig. 11 and the resulting velocities in Fig. 12. As expected, and in contrast to the bare hull condition, Fig. 11 shows a static pressure difference across the flow indicating a curvature of the streamlines. Also note the unusual shape of the total pressure profiles in Fig. 11. In some cases the total pressure is higher near the wall than it is further away from the wall. Apparently there is

15

some sort of secondary flow that is sweeping higher energy flow from the outer edge of the boundary layer, or even the free stream, into the inlet and some of the lower energy flow out of the inlet. As will be seen later when discussing Reynolds' Number corrections the ingested layer is about 1/2 of the boundary layer thickness at model scale and is estimated to be somewhat larger than a boundary layer thickness at full scale. In either case a longitudinal vorticity could readily be developed from the stretching of the boundary layer vorticity by the distortion of the flow approaching the inlet. Such a large effect as that indicated on Fig. 11 is, however, surprising. Table 8 shows the average velocities obtained under powering conditions. The velocities are considerably higher than those obtained under bare hull conditions. Furthermore, the energy-averaged velocities are higher than those in the inlet as they must be.

| SPEED | $V_{mass}/V_S$ | $V_{mom}/V_S$ | $V_{energy}/V_S$ |
|---|---|---|---|
| 12 | .827 | .860 | .876 |
| 20 | .831 | .865 | .880 |
| 28 | .836 | .869 | .884 |

**TABLE 8**

**Self-Propelled Hull Capture Area Velocities**

The inlet efficiency defined as

$$\eta_{nlet} = \frac{(V_{energy}^2)_{INLET}}{(V_{energy}^2)_{CAPTURE}}$$

using the propelled hull energy-averaged velocities at the capture are shown in Table 9. Data from Fig. 6-20 of Ref. 3, which were taken in a water tunnel with zero pressure gradient, is included as a comparison. That data have considerable scatter but it does seem to have significantly less variation with the inlet velocity ratio than does the data of these tests. Both sets of data show the inlet efficiency increasing with increasing inlet velocity ratio.

16

| SPEED | IVR | $\eta_{inlet}$ | $\eta_{inlet}$- [Ref. 3] |
|---|---|---|---|
| 12 | 1.024 | .66 | .77 |
| 20 | 1.088 | .80 | .79 |
| 28 | 1.210 | .87 | .81 |

## TABLE 9
### INLET EFFICIENCIES


## POWERING

Powering estimates for the integrated hull VMP propulsor were determined by using the energy averaged velocities in the jet and in the pump inlet area, an appropriate pump efficiency and a passage loss coefficient. The self-propulsion data were determined in the conventional manner with an offset to simulate full-scale resistance. However, the Reynolds' Number effects on the hull boundary layer and, consequently, the inflow are not included in the tests and so had to be estimated.


### PUMP EFFICIENCY AND PASSAGE LOSSES

Since the inlet area rather than the capture area was used as the upstream station for the energy integration, the inlet losses are inherently included in the data. There is practically no passage associated with the VMP design other than the volute exit to rectangular transition piece and the nozzle exit. A passage loss coefficient of .05 (losses equal to 5% of a passage velocity head) was arbitrarily used in this analysis.

| SHIP SPEED | $c_H/c_m^2$ x $10^{-6}$ |
|---|---|
| 12 | 1.64 |
| 20 | 1.59 |
| 28 | 1.85 |

## TABLE 10
### Pump Operating Point

17
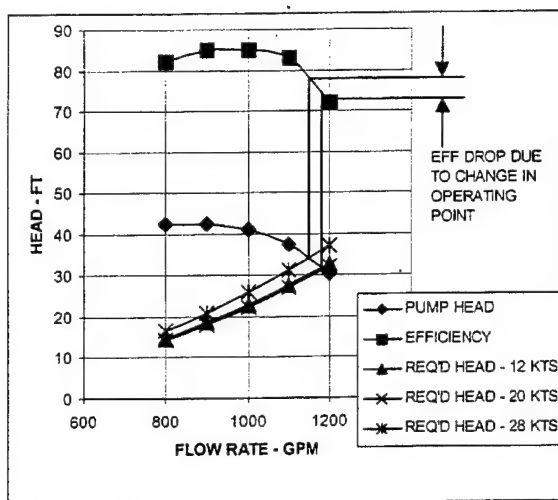
**FIG. 13**
**Efficiency Drop Due To Change in**
**Operating Point**

A model of the VMP as conceived at the time was built and tested by Ingersoll-Dresser [Ref. 4]. That model was meant to simulate a 50,000 HP design rather than the current 25,000 HP unit. The 50,000 HP design had a diameter constraint that required significant folding of the volute. A more recent 25,000 HP concept design for the same hull allows for a more conventional volute and , presumably, a more efficient design. Nevertheless, the 50,000 HP data is the only data available at the present time. Ingersoll-Dresser states that "full size --- pump efficiency of between .80 and .85 could be expected." A pump efficiency of 0.85 at 28 knots was assumed in this analysis. However, the pump efficiency would normally change, at least a little, with ship speed. The main reasons for this change would be Reynolds' Number effects and variations in the pump operating point (essentially angle of attack on the rotor blade). Table 10 shows the variation in the ratio of the head coefficient to the square of the mass flow coefficient, which is an indicator of the pump operating point. Waterjets generally show very little variation in the pump operating point. The variation that does occur is the result of the interaction of several effects, however for units with jet velocity ratios typical of waterjets the inlet losses are the primary contributor. The variation shown in Table 10 is a little more than what was expected and would have a significant effect on pump efficiency. A part of the pump curve from the Ingersoll-Dresser report [Ref. 4] is included as Fig. 13. An estimate of the required passage head at 12, 20 and 28 knots is also included thus yielding the operating points at these three speeds. These operating points lie in a region where the efficiency is dropping rapidly. An efficiency loss of 4% at 12 knots and 6% at 20 knots relative to the 28 knot condition is indicated. A pump designed to operate on the flatter part of the efficiency curve would be more appropriate to this application.

Fig. 14-17 in Stepanoff's book [Ref. 5] indicates a decrease in efficiency of about 3% for a Reynolds' Number range corresponding to the difference between 12 and 28 knots. The pump efficiencies were therefore taken as shown in Table 11.

18

| SPEED | BASE EFF | Oper. Point Corr. | Re NO. Corr | Pump Eff |
|-------|----------|-------------------|-------------|----------|
| 12 | .85 | .04 | .03 | .78 |
| 20 | .85 | .06 | .015 | .775 |
| 28 | .85 | 0. | 0. | .85 |

<div align="center">

**TABLE 11**

**Pump Efficiencies**

</div>

## REYNOLDS' NO. CORRECTIONS

The towing tank self-propulsion data were taken with standard compensation for the full-scale ship resistance but did not include any Reynolds' Number adjustment for the ingested hull boundary layer thickness. Reynolds' Number corrections will be addressed assuming a zero pressure gradient along the bottom of the ship and, as such, are directly applicable only to the unpropelled condition. The turbulent boundary layer growth is given by

$$\frac{\delta}{l} = .37(\frac{V_s l}{\nu})^{-0.2}$$

where $l$ should be the axial distance from the leading edge of the ship to the capture area. However, the full length of the ship will be used here. The expressions for the various average velocities are different depending on whether or not the ingested thickness is greater or less than the boundary layer thickness. Assuming a $1/7^{th}$ power velocity distribution it can readily be shown that

$$\frac{y_0}{\delta} = (\frac{8}{7}\frac{c_Q}{\delta/l})^{7/8} \qquad \frac{y_0}{l} \leq 1$$

$$\frac{y_0}{\delta} = \frac{c_Q}{\delta/l} + \frac{1}{8} \qquad \frac{y_0}{l} \geq 1$$

where $y_0$ is the thickness of the ingested layer and $c_Q$ is a flow coefficient defined as

$$c_Q = \frac{Q}{V_s l w}$$

19

where w is the average width of the ingested layer. It will be assumed that this flow coefficient is independent of the Reynolds' Number. The thickness of the ingested layer at both model-scale and full-scale Reynolds' Numbers are shown in Table 12.

| SHIP SPEED | $c_{Q \times 10^3}$ | MODEL-SCALE | | FULL-SCALE | |
|---|---|---|---|---|---|
| | | $Re \times 10^{-6}$ | $y_o/\delta$ | $Re \times 10^{-8}$ | $y_o/\delta$ |
| 12 | 5.98 | 6.93 | .479 | 8.67 | 1.115 |
| 20 | 6.54 | 11.56 | .582 | 14.45 | 1.326 |
| 28 | 7.02 | 16.18 | .650 | 20.23 | 1.503 |

**TABLE 12**

**Calculated Ingested Thickness**

The width of the elliptical capture area used above was close to 3.0 inches with little variation with ship speed so that was used here. Again assuming a 1/7$^{th}$ power velocity distribution, the various average velocities are

$$\frac{V_{mass}}{V_S} = \frac{7}{8}(\frac{y_o}{\delta})^{1/7} \qquad \frac{y_o}{\delta} \leq 1$$

$$= \frac{\delta}{y_o}[\frac{y_o}{\delta} - \frac{1}{8}] \qquad \frac{y_o}{\delta} \geq 1$$

$$\frac{V_{mom}}{V_S} = \frac{8}{9}(\frac{y_o}{\delta})^{1/7} \qquad \frac{y_o}{\delta} \geq 1$$

$$= \frac{(\frac{y_o}{\delta} - \frac{2}{9})}{(\frac{y_o}{\delta} - \frac{1}{8})} \qquad \frac{y_o}{\delta} \geq 1$$

$$(\frac{V_{energy}}{V_S})^2 = \frac{8}{10}(\frac{y_o}{\delta})^{2/7} \qquad \frac{y_o}{\delta} \leq 1$$

$$= \frac{(\frac{y_o}{\delta} - \frac{3}{10})}{(\frac{y_o}{\delta} - \frac{1}{8})} \qquad \frac{y_o}{\delta} \geq 1$$

The resulting average velocities are shown in Table 13. The velocities measured along the centerline of the inlet at the unpropelled condition are considerably less than the values in Table 12; however, the off-centerline values appear to be more comparable.

| SHIP | MODEL-SCALE | | | FULL-SCALE | | |
|------|-------------|--|--|------------|--|--|
| SPEED | $V_{mass}/V_S$ | $V_{mom}/V_S$ | $V_{energy}/V_S$ | $V_{mass}/V_S$ | $V_{mom}/V_S$ | $V_{energy}/V_S$ |
| 12 | .788 | .800 | .805 | .888 | .902 | .907 |
| 20 | .810 | .823 | .828 | .906 | .919 | .924 |
| 28 | .823 | .835 | .841 | .917 | .929 | .934 |

**TABLE 13**

**Calculated Capture Area Average Velocities**

The full-scale average velocities are all about 0.10 higher than the model-scale velocities. The model-scale to full-scale Reynolds' Number correction will be made by simply adding 0.10 to the energy-averaged velocities at both the inlet and jet areas.


**POWERING RESULTS**

The powering results are shown in Table 14 and Fig. 2 on page 4. The data labeled INFERRED FROM TESTS correspond to the data obtained in the test program with the pump efficiencies and passage loss coefficient described above. These self- propulsion data include an offset for the full-scale ship frictional resistance but do not include any Reynolds' Number correction for the hull boundary layer. The data labeled Re NO. CORR. includes the hull boundary layer correction. This was accomplished by simply adding 0.10 to the energy-averaged velocities at both the inlet area and the jet area as described above. The data labeled PROP are from Cusanelli and Karafiath's recommendations (see Appendix II) for the DDG 51 powering performance that would give the most realistic comparison for these tests. Both the INFERRED FROM TESTS and Re NO. CORR power levels are below the propeller variant at 12 and 28 knots and they bracket the propeller variant at 20 knots.

| SPEED | INFERRED FROM TEST | Re NO. CORR | PROP[*] |
|---|---|---|---|
| 12 | 1826 | 1993 | 2634 |
| 20 | 12,520 | 13,544 | 13,363 |
| 28 | 42,887 | 46,121 | 49,862 |

\* Model 5513 @ 8500T – ATD Prop $c_a$=0.0004(from Table 5 in Appendix II)

**TABLE 14**

**Powering Results**

Table 15 shows the composition of the power at INFERRED FROM TESTS conditions.  The increment for the frictional losses is small because the inlet losses are already included in the ideal power.  The total power is obtained by dividing the $HP_{ideal}$ +$HP_{friction}$ by the pump efficiency from Table 11.

| SPEED | $HP_{ideal}$ | $HP_{ideal}$ +$HP_{friction}$ | $HP_{total}$ |
|---|---|---|---|
| 12 | 1375 | 1424 | 1826 |
| 20 | 9456 | 9703 | 12,520 |
| 28 | 35,728 | 36,454 | 42,887 |

**TABLE 15**

**Composition of  'INFERRED FROM TESTS' Power**
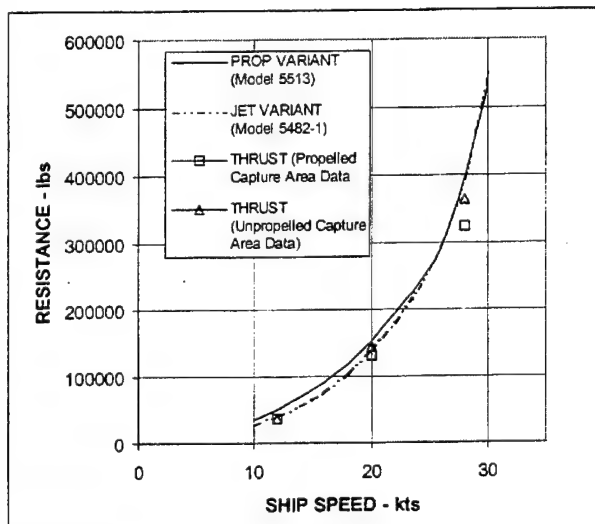


**FIG. 14**
**VMP/Propeller Resistance Comparisons**

The unpropelled resistance of the waterjet variant, Model 5482-1, with the 5-hole probe simulating the bilge keel drag in place has already been compared to its parent, Model 5415, in Fig. 3 on page 7.  However, Cusanelli and Karafiath have pointed out that Model 5513 is more representative of the full scale DDG 51. The unpropelled resistance of both Model 5513 (as provided by Cusanelli and Karafiath in Table 5 of Appendix II) and Model 5482-1 with the velocity probe in place, is shown in Fig. 14. The Reynolds' Number corrected propulsor

thrust as obtained by the momentum averaged jet and capture area velocity difference is also included. Results obtained with both the unpropelled and the propelled capture area are included. As pointed out previously, the unpropelled capture area data was not consistent with the inlet area data and so the propelled data, the squares on Fig. 14, is probably the more realistic. The waterjet variant had less resistance than the propeller variant at the lower speeds but about the same at the higher speeds. The waterjet thrust and the unpropelled resistance of the waterjet hull were about the same at 12 and 20 knots, but at 28 knots the waterjet thrust was significantly less than the unpropelled resistance of either hull. It appears that the integrated design had a major effect in achieving a strong favorable propulsor/hull interaction at the ship speed for which it was designed.

The hydraulic efficiency, the ideal efficiency and the propulsor/hull interaction can be obtained by substituting the appropriate average velocities in the equations given above. The results are shown in Table 16. The hydraulic efficiency is higher than what might be expected because the inlet losses are included in the ideal efficiency. Both the ideal efficiency and (1-t) were evaluated using the self-propelled data at the capture area and their uncertainties are comparable to the uncertainties associated with the capture area. However, the momentum thrust appears in the numerator of one and the denominator of the other so their product is not dependent on the capture area uncertainties. The propulsor/hull interaction, (1-t), is essentially the same information as shown in Fig. 14.

| SPEED | $\eta_P$ | $\eta_H$ | $\eta_I$ | 1-t[*] | $HP_{eff}$[*] | HP |
|-------|-------|-------|-------|-------|-------|-------|
| 12 | .78 | .966 | 1.098 | .960 | 1450 | 1826 |
| 20 | .775 | .975 | .852 | 1.034 | 8328 | 12,520 |
| 28 | .85 | .980 | .820 | 1.136 | 33,288 | 42,887 |

*Effective horsepower from Table III-6 in Appendix III

**TABLE 16**

**Various Efficiencies and Coefficients**

Since the drag of the ship increases with ship speed so does the non-dimensional mass flow rate. Consequently, the stagnation point on the downstream lip of the inlet will move downstream as the speed increases thereby increasing the pressure on the aft end of the hull. This would explain the increase of (1-t) with ship speed. Nevertheless, the value for (1-t) at 28 knots is surprisingly high. It suggests that both a favorable propulsor/hull interaction and a reduction in the wave drag are occurring. If this is true it is very significant and gives an indication of what can be accomplished by an integrated propulsor/hull design.

## POWERING ANALYSIS UNCERTAINTIES

In this particular set of experiments the uncertainty is due primarily to the analysis rather than the collection of the data. All of the powering analyses involved integration of the collected data, which tends to smooth out the random data collection errors. Most of the uncertainty arises in determining the mass flow rate from the measurements at the inlet area, from the hull flow Reynolds' Number corrections and from the assumed pump efficiency.

The flow rate was obtained from a Simpson's Rule integration of the measured velocities at the circular inlet area. Most of the uncertainty arises from the manner in which the outer ring is handled. Simpson's Rule assumes a linear distribution of the data between the mesh points whereas the decrease of the velocity from the outermost measuring radius to its zero value at the wall is decidedly non-linear. This situation was handled in the analysis that has already been presented by taking the average velocity in the outermost ring to be ¾ of the outermost

| Weighting | $V_{model}$ = 4.065 ft/sec | | $V_{model}$ = 6.775 ft/sec | | $V_{model}$ = 9.485ft/sec | |
|---|---|---|---|---|---|---|
| | $Q - ft^3/sec$ | % diff | $Q - ft^3/sec$ | % diff | $Q - ft^3/sec$ | % diff |
| ½ | .226 | -5.0 % | .377 | -4.3 % | .595 | -4.3 % |
| ¾ | .238 | 0 % | .394 | 0 % | .622 | 0 % |
| 1 | .250 | +5.0% | .411 | +4.3 % | .650 | +4.5 % |

**TABLE 17**

**Flow Rate Uncertainties**

24

measurement rather than the ½ that would normally be used for a linear distribution. A sensitivity analysis was performed by allowing the average value in the outermost ring to range from ½ to 1 times the outermost measurement. This more than covers the possible range and so can be thought of as including all of the other integration errors that might also arise. The results at the three test speeds are shown in Table 17. At the most one would expect the uncertainty in the flow rate to be +/- 5%. Since the power required is directly proportional to the flow rate, one would expect that the uncertainty in the power requirement due to flow rate uncertainties also to be +/- 5%.

A pump efficiency of 85% was used in the analysis. This was a result of model tests of a unit designed and tested by Ingersoll-Dresser Pump Corp. scaled to the full scale Reynolds' Number based on their past experience. The specific speed in units of RPM $(GPM)^{1/2}$ / $Ft^{3/4}$ at the 28 knot operating condition would be in the neighborhood of 4000 and the flow rate would be slightly more than 860,000 GPM. A specific speed of 4000 is typical of a mixed flow pump and efficiencies of over 90% are characteristic of such pumps at high flow rates such as this. The often cited curve of efficiency verses specific speed on which this statement is based can be found as Fig. 5.1 on page 76 of Stepanoff's book [Ref. 5] and also in Fig. 29 of Allison [Ref. 6]. The pump volute is of an unusual design and this was the first attempt at that design. Continued development can reasonably be expected to lead to an efficiency in the neighborhood of 90%.

As mentioned earlier the corrections for the hull Reynolds' Number effects are very approximate. The analysis was based on a zero pressure gradient flow over a smooth surface whereas there is a pressure gradient along the hull and the surface is not smooth. If anything both the pressure gradient and the rough surface would thicken the boundary layer and so the analysis is probably on the conservative side. However, the flow approaching the inlet is highly three dimensional and it is not very likely that it can be adequately represented with any simple, one dimensional model. Methods for correcting for hull flow effects on propulsion units using boundary layer intakes over such large Reynolds' Number variations as in these tests should be addressed using the 3D RANS codes presently available at NSWCCD.

The uncertainties in the jet velocities was discussed in the section titled Jet Velocities on page 14. These arise because of the uncertainty in the location of the edges of the jet; they are not very large.

## STATIC PRESSURE MEASUREMENTS

Static pressure measurements were made at a number of locations both on the hull and inside the duct. Data were obtained at seven ship speeds and at several pump RPMs at each ship speed. The location of the measuring stations is shown in Fig. 15. The
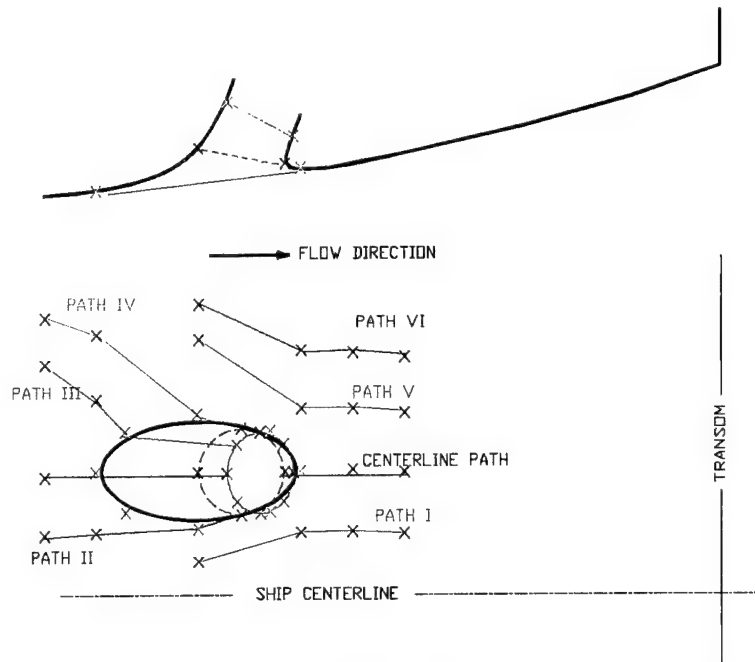


**FIG. 15**
**Surface Pressure Measuring Stations**

upper part of Fig. 15 is a longitudinal section through the center of the inlet; the lower part is a bottom view of the hull. The drawing is to scale and both the centerline of the ship and the location of the transom are indicated. The hull measuring stations are shown with a black x. These stations were chosen to lie along estimates of surface flow lines as obtained from an earlier potential flow solution for the hull flow. These estimated flow lines are shown in various colors on Fig. 15 and are labeled as CENTERLINE PATH and PATH I through PATH VI. The surface pressures within the duct were obtained around the periphery at three planar cuts. The first was at the intersection of the duct and the hull; these measuring stations are shown with green marks on the lower part of Fig. 15

and the planar cut with a green line on the upper part of the figure. The second and third cuts are shown with blue and magenta lines on the upper part of Fig. 15 and with blue and magenta marks connected with blue and magenta lines on the bottom.

## INLET CENTERLINE PRESSURES

Pressure coefficients along the centerline of the inlet, the red line marked CENTERLINE PATH in Fig. 15, at model speeds of 4.09, 6,78 and 9.49 ft/sec are shown in Figs. 16, 17 and 18. These ship speeds correspond to full-scale ship speeds of 12, 20 and 28 knots. The abscissa is in model scale inches using the upstream edge of the inlet as the zero. The contour of the inlet is also shown and the self-propulsion RPM indicated to help interpret the data. The transom is located at a longitudinal location of 24 inches.
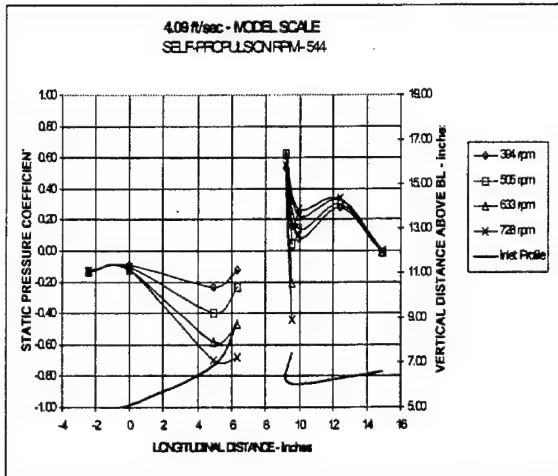


**FIG. 16**
**Centerline Pressures at 4.09 Ft/Sec**
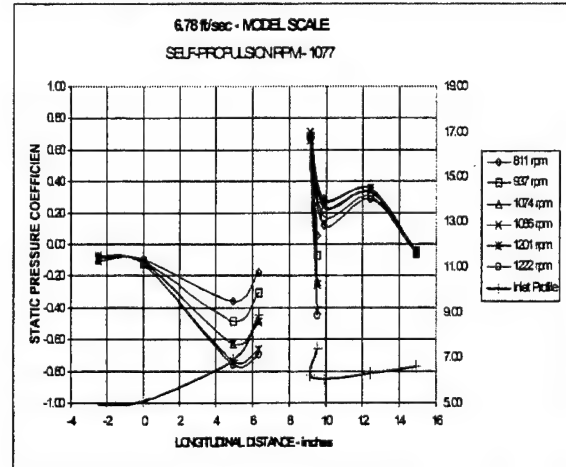


**FIG. 17**
**Centerline Pressures at 6.78 Ft/Sec**

The minimum pressure in the inlet decreases as the pump RPM, and consequently the flow rate , increases as would be expected. The pump RPM is directly related to the inlet velocity ratio. The inlet velocity ratio corresponding to the lowest RPM is 0.74 at 4.09 ft/sec (Fig. 16), 0.82 at 6.78 ft/sec and 1.03 at 9.47 ft/sec. There is no evidence of any flow separation even at the relatively low inlet velocity ratio of 0.74 (waterjets customarily operate at an inlet velocity ratios of 0.80 and above) corresponding to a pump speed of 394 RPM in Fig. 16.

27

The static pressures at the RPM closest to the self-propulsion RPM are shown in Fig. 19. The stagnation point on the downstream edge of the inlet is inside of the inlet at all ship speeds. The valley at an axial location of 10.0 inches results from the acceleration of the flow as it
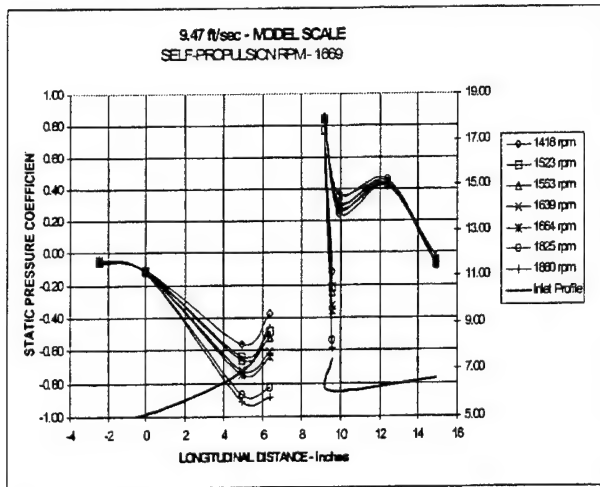


**FIG. 18**
**Centerline Pressures at 9.47 Ft/Sec**
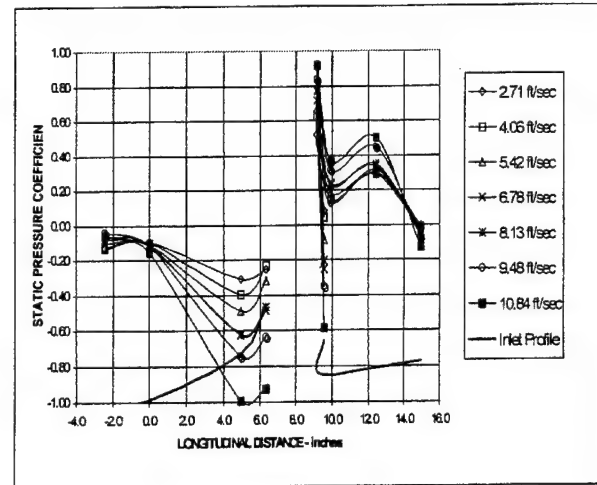


**FIG. 19**
**Centerline Pressures at Self- Propulsion**

negotiates its way around the downstream edge of the inlet. A more generous rounding of this edge could probably eliminate it and possibly increase the (1-t). The static pressure downstream of the inlet is above atmospheric pressure, at least for a distance comparable to the inlet size. This is in contrast to the pressure distribution on the aft end of a propeller driven ship, which is usually less than the free stream pressure. This altered pressure distribution on the aft end of the ship affects both the form drag and the wave drag and is part of the reason for the favorable propulsor/hull interaction. The interaction between the hull flow and the underwater discharge also affects the form and wave drag, but no diagnostic data were obtained in these experiments.
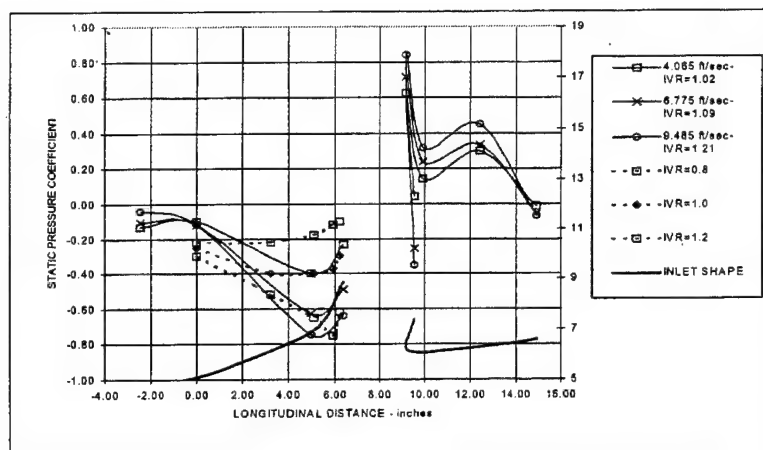
**FIG. 20**
**Pressure At Self-Propulsion Compared to Data of Ref. 3**

Fig. 20 shows the three curves from Fig. 19 that correspond to full scale ship speeds of 12, 20 and 28 knots but with some results from the tests of Ref. 3 superimposed. The dashed lines are from Ref. 3 and correspond to inlet velocity ratios (IVR) of 0.8, 1.0 and 1.2. Both the trends and the levels are consistent with each other. There is no evidence of separation from either set of data, even at the lower inlet velocity ratios where separation is more likely to occur.

## OFF CENTERLINE STATIC PRESSURES

The hull static pressures measured along the paths labeled PATH I through PATH VI on Fig. 15 at a model speed of 9.49 ft/sec are shown in Figs. 21 through 26. The distributions at the other ship speeds were very similar. The abscissa is the longitudinal distance in model scale inches measured from the upstream edge of the inlet just as in the previous figures.

Figs. 21, 25 and 26 show that there is very little change in the static pressure and very little dependence on pump RPM along the three paths that bypass the inlet; that is PATH I, PATH V and PATH VI. The pressure distribution along PATH II, which is not very far from the slot centerline, is similar to the centerline distribution. Again, there is no indication of flow separation at any pump speed. The distribution along PATH III in Fig. 23 is inconclusive because there was no point along this path in the vicinity of the minimum pressure location. The distribution along PATH IV in Fig. 24 is similar to the centerline distribution but with reduced gradients as would be expected. PATHs II and IV are estimates of the limits of the surface flow into the inlet.

29
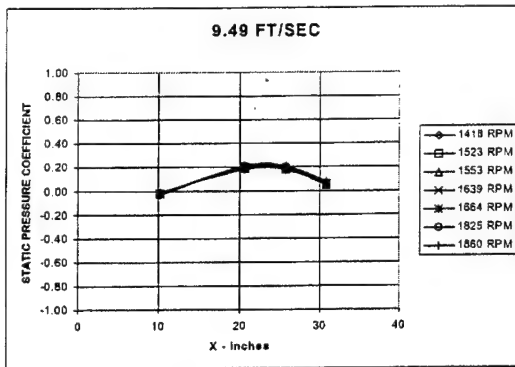
**FIG. 21**
**Static Pressure Distribution PATH I**
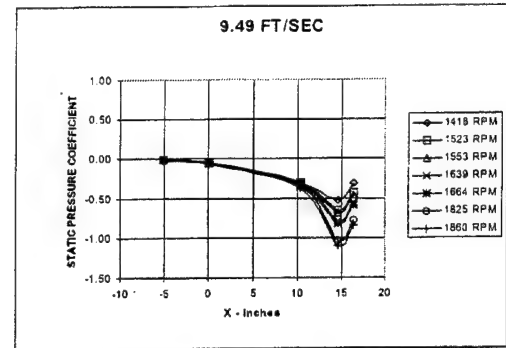


**FIG. 22**
**Static Pressure Distribution PATH II**
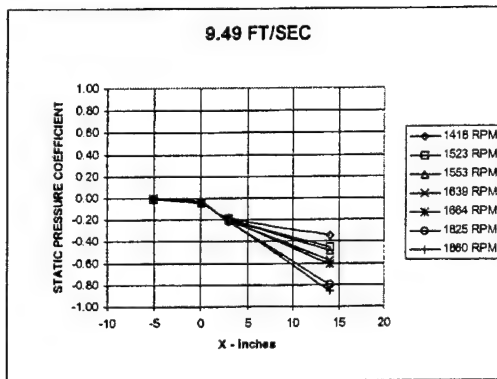


**FIG. 23**

**Static Pressure Along PATH III**
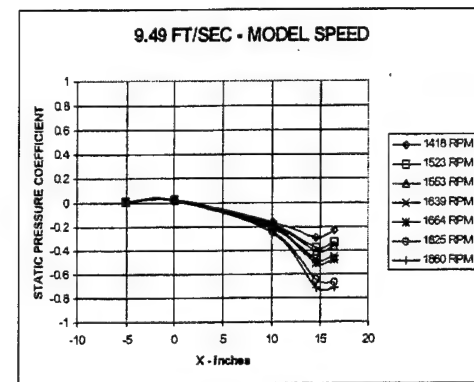


**FIG. 24**
**Static Pressure Along PATH IV**
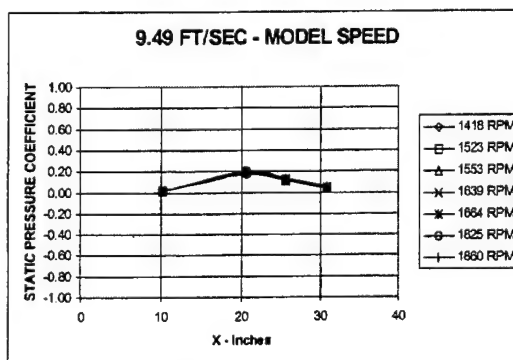


**FIG. 25**
**Static Pressure Along PATH V**
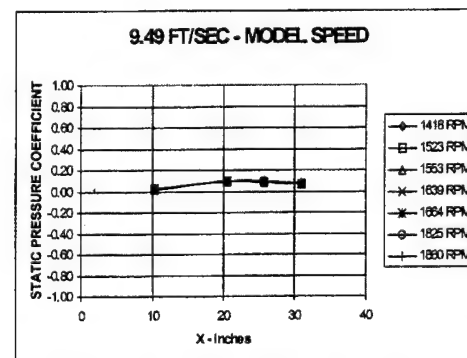


**FIG. 26**
**Static Pressure Along PATH VI**

## DUCT PRESSURES

Static pressures were also measured around the outside of the duct at three locations as shown in Fig. 15. The first location was not actually inside of the duct but around the elliptical intersection of the duct with the hull surface. Fig. 27 shows the pressures at those stations, which are the green marks of Fig. 15. The angular position marked as 0° is on the downstream edge of the inlet. This point is a little downstream of the stagnation point and the dip at 0° is the same flow acceleration around the downstream lip that was seen on the centerline pressures. The part of the curve that lies between the two valleys at approximately +/- 90° shows the pressures near the stagnation line where non-surface flow is entering the inlet. The part of the curve below approximately −90° and above +90° shows where surface flow is entering the inlet. Figs. 28 and 29 show the static pressures inside of the duct. Fig. 28 is at a location a little inside of the stagnation point; there is considerable circumferential variation at this location as there must be if it is in the stagnation region. Fig. 29 is at a location deeper within the duct. There is not very much circumferential variation at this location and the pressure variation with pump RPM, and hence flow rate and inlet velocity ratio, is obvious.



**FIG. 27**
**Static Pressures Around Duct Inlet**
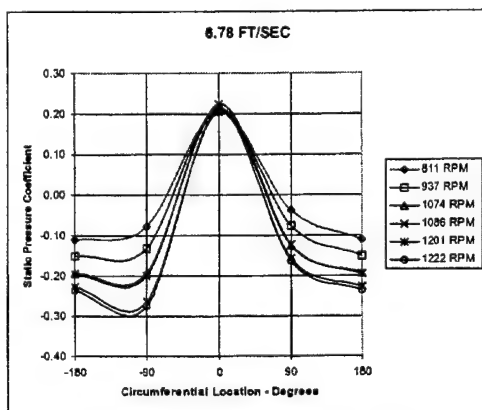


**FIG. 28**
**Static Pressures Inside Duct**
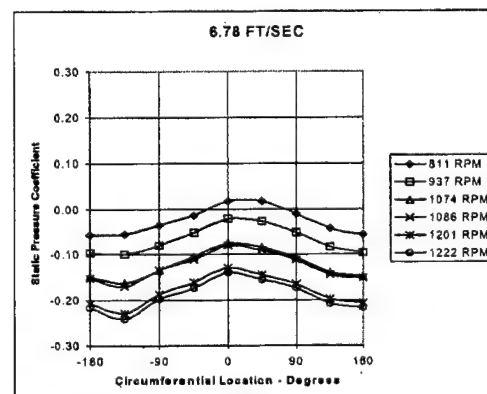


**FIG. 29**
**Static Pressures Deep Inside Duct**

31

# CAVITATION

Preventing cavitation on any type of surface ship at speeds greater than something like 25 knots is a difficult problem with any type of propulsor. Waterjets have an advantage in that the inlet flow can be diffused and, consequently, the pressure entering the rotor increased. Conceptually, a waterjet can be designed to be cavitation free at quite high ship speeds. The data of this experiment shows that the inlet itself would be cavitation free at over 30 knots. Using the blades surface pressure diagrams from the Ingersoll-Dresser report [Ref. 4] in conjunction with the results of these experiments indicates that blade surface cavitation would occur between 24 and 25 knots with this inlet configuration and pump design. However, the inlet velocity ratio at self-propulsion and 28 knots was 1.21 whereas waterjets usually operate under design conditions at approximately 0.8. Inlet velocity ratios above 1.0 indicate an acceleration (decreasing pressure) of the inlet flow and values less than 1.0 indicate a deceleration (increasing pressure) of the inlet flow. Increasing the inlet area by approximately 30% would result in an inlet velocity ratio at 28 knots of 0.85, well within acceptable limits, and raise the cavitation free ship speed to 28 knots.

The depth at the inlet area required to prevent cavitation in the inlet is

$$h = \frac{V_S^2}{2g}(-c_{p\text{-}static})$$

In this equation $c_{p\text{-}static}$ is the static pressure coefficient at the inlet. Since there was a variation of the static pressure across the inlet area the lowest value was used in this equation. The depth required to prevent blade surface cavitation on the blade is

$$h = \frac{V_S^2}{2g}\{c_{p\min}[(\frac{V_I}{V_S})^2 + (\frac{\pi}{J})^2] - c_{p\text{-}static}\} - 32\,ft$$

In this equation the mass averaged velocity at the inlet should be used for $V_I$ and the advance ratio, J, and blade minimum pressure coefficient, $c_{p\min}$, corresponding to the candidate propulsor, the VMP in this case, should be used. This equation accounts for the blade surface cavitation that would occur as the blade sweeps through the more or less uniform velocity part of the inlet area.

No account is made for the leading edge cavitation that occurs as the blade passes through the lower velocity part of the inlet area; it would be more severe and would require a greater depth.
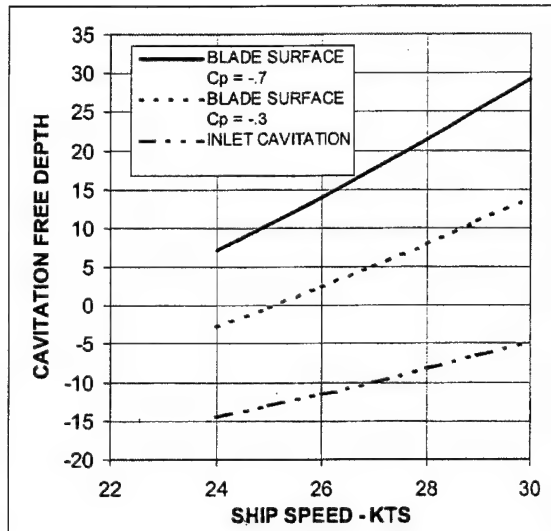


**FIG. 30**
**Estimated VMP Cavitation**

Fig. 30 shows the required cavitation depth as a function of ship speed. The curves marked "BLADE SURFACE $c_p$ = -.7" and "INLET CAVITATION" were obtained by using a value of $-0.7$ for $c_p$, which was the lowest value for the pressure coefficient in the inlet at 28 knots. The mass averaged velocity in the inlet at 28 knots was used for $V_I/V_S$. These values depend on the ship speed, but that effect was neglected. Using 8 feet as the submergence, these curves indicate that the inlet itself would not cavitate until well above 30 knots. Assuming the same 8 foot submergence depth, blade surface cavitation would occur at between 24 and 25 knots for this particular inlet configuration and pump design. The advance ratio and $c_{pmin}$ were taken from the Ingersoll-Dresser design [Ref. 4].

The designer can control the cavitation, at least to some degree, by the choice of inlet area. If the inlet area is increased the pressure coefficient also increases and the inlet velocity decreases. Both of these tend to decrease the cavitation free depth. The curve on Fig. 30 marked "BLADE SURFACE – $c_p$ = -.3" is the required depth if the inlet where enlarged so that the pressure coefficient increased to $-0.3$, which is what it would take to eliminate the blade surface cavitation at 28 knots and an 8 foot submergence. This would require either an increase in the inlet area of approximately 30% or an increase in the submergence of the inlet or some combination of both.

The inlet velocity ratio at a full scale speed of 28 knots was 1.21 as compared to the 0.80 typical of common waterjet practice, so the inlet area could easily be increased considerably. Increasing the inlet area by 30% would result in inlet velocity ratios of .72, .76 and .85 at ship speeds of 12, 20 and 28 knots. The .85 at 28 knots is well within the acceptable range, but the .72

33

and .76 at 12 and 20 knots are a little low and there is, potentially, a danger of flow separation in the inlet at these speeds. However, the centerline pressure distributions shown in Figs. 16 and 17 do not show any indication of flow separation even at the low pump speeds. In Fig. 16, which corresponds to a full scale ship speed of 12 knots, a pump speed of 380 RPM corresponds to an inlet velocity ratio of .72; in Fig. 17 a pump speed of 753 corresponds to an inlet velocity ratio of .76.

## CONCLUSIONS

1. Model tests suggest that the Reynolds' Number corrected power required to propel the full scale ship at 12 and 28 knots is less than the power required to propel an equivalent ship using an open propeller and comparable at 20 knots.

2. The flow upstream of the inlet is significantly effected by the operation of the propulsor and secondary flows are developed that mix the flow in a complicated way and make any analysis at this measuring station difficult to accomplish.

3. The inlet recovery varied from 66% at 12 knots where the inlet velocity ratio was 1.02 to 87% at 28 knots where the inlet velocity ratio was 1.21.

4. The value of (1-t) ranged from .96 at 12 knots through 1.03 at 20 knots and up to 1.14 at 28 knots. The relatively high value of 1.14 at 28 knots suggests that considerable gains could be achieved from an integrated propulsor/hull design.

5. Static pressure measurements along the hull were in good agreement with the measurements of Barr, Bohn and Bateman given in Ref. 3.

6. Static pressure measurements along the hull did not show any evidence of flow separation in the inlet even at pump speeds corresponding to low inlet velocity ratios.

7. The static pressure distribution on the hull surface downstream of the inlet was above the free stream static pressure thus contributing to the positive thrust deduction.

8. The inlet stagnation point was inside of the inlet and there was a noticeable dip but no flow separation in the pressure distribution as the downstream flow accelerated back around the downstream edge of the inlet.

## RECOMMENDATIONS

It is recommended that:

1. development of the inlet and surrounding hull geometry be continued with particular emphasis on lower inlet velocity ratios and more uniform inlet velocity distributions;

2. a study of the inlet geometry and other factors involved in increasing the cavitation free ship speed be initiated;

3. the pump design be revised and further developed with particular emphasis on placing the design point on the flat part of the efficiency curve;

4. a study of the design techniques for and the performance characteristics of pump volutes of the type required for the VMP application be undertaken;

5. based on the favorable propulsor/hull interaction effect obtained with this first attempt, the concept of an integrated propulsor/hull design be pursued further.

6. a method for correcting for hull flow Reynolds' Number effects be developed possibly using the 3D RANS codes now in use at NSWCCD.

## ACKNOWLEDGEMENTS

(THIS PAGE INTENTIONALLY LEFT BLANK)

# REFERENCES

1. Dai, Charles; Peterson, Frank and McMahon, Jack, "Development of a Vertical Motor Propulsor", SNAME Propellers/Shafting '97 Symposium, Sept. 23-24,1997

2. "Waterjets Group – Final Report and Recommendations to the 21$^{st}$ ITTC"

3. Barr, Roderick, Bohn, Jeffrey, and Bateman, "Water Channel Tests Of Three Inlet Designs For the Vertical Motor Propulsor", Hydronautics Research, January 1995

4. Sloteman, Donald P., "Vertical Axis Motor Propulsor (VAMP) Bench Scale Model Testing", Ingersoll-Dresser Pump Company, January 3, 1998

5. Stepanoff, A. J., "Centrifugal and Axial Flow Pumps", 1948

6. Allison, John L., "Marine Waterjet Propulsion", SNAME Transactions, Vol. 101, pp. 275-335, 1993

(THIS PAGE INTENTIONALLY LEFT BLANK)

**APPENDIX I**
**Resistance Data for Model 5415**

| Title: | DDG-51 | Friction Line: | ITTC | Laboratory: | NSWC |
| Model Name: | 5415 | Working Fluid: | Fresh Water | Code Name: | |
| Model Weight: | 1210.00 lbs | Water Temperature: | 66.0°F | Code Number: | |
| Longitudinal C.G, Ref.: | From Mid Ship | Water Density: | 1.937 sl/ft^3 | Experimenters: | |
| Longitudinal C.G.: | -13.23 in | Water Viscosity: | 1.110E-05 ft^2/sec | Facility: | Shallow Basin |
| Frontal Area: | 0.00 sqin | Air Temperature: | 74.0°F | Carriage: | Carriage 1 |
| Stimulator: | Studs | Air Density: | 2.311E-03 ft^2/sec | Test Period: | |
| Stimulator Penalty: | 0.000E+00 | Air Viscosity: | 1.657E-04 ft^2/sec | Sponsor: | |
| Correlation Allowance: | 4.000E-04 | Assumed Aero Drag Coef.: | 0.000 | Job Order Number: | |

| Hull Speed Vm (fps) | Total Resistance Rtm (lbs) | Areo Resistance Ram (lbs) | Running Trim Pm (deg) | Heave Disp Zm (in) | Wetted Length Fn WLfm (in) | Wetted Length Rn WLrm (in) | Wetted Surface WSAm (sqft) | Froude Number Fn | Reynolds Number Rnm | Total Drag Coef Ctm | Friction Coef Cfm | Residual Coef Cr |
|---|---|---|---|---|---|---|---|---|---|---|---|---|
| 0.00 | 0.00 | 0.00 | - | - | 225.24 | 225.24 | 51.96 | 0.000 | 0.000E+00 | - | - | - |
| 0.34 | 0.03 | 0.00 | - | - | 225.24 | 225.24 | 51.96 | 0.014 | 5.729E+05 | 6.055E-03 | 5.311E-03 | 7.443E-04 |
| 0.68 | 0.12 | 0.00 | - | - | 225.24 | 225.24 | 51.96 | 0.028 | 1.146E+06 | 5.194E-03 | 4.552E-03 | 6.418E-04 |
| 1.02 | 0.25 | 0.00 | - | - | 225.24 | 225.24 | 51.96 | 0.041 | 1.719E+06 | 4.775E-03 | 4.181E-03 | 5.934E-04 |
| 1.36 | 0.42 | 0.00 | - | - | 225.24 | 225.24 | 51.96 | 0.055 | 2.291E+06 | 4.512E-03 | 3.945E-03 | 5.670E-04 |
| 1.69 | 0.63 | 0.00 | - | - | 225.24 | 225.24 | 51.96 | 0.069 | 2.864E+06 | 4.332E-03 | 3.775E-03 | 5.565E-04 |
| 2.03 | 0.87 | 0.00 | - | - | 225.24 | 225.24 | 51.96 | 0.083 | 3.437E+06 | 4.206E-03 | 3.645E-03 | 5.617E-04 |
| 2.37 | 1.17 | 0.00 | - | - | 225.24 | 225.24 | 51.96 | 0.096 | 4.010E+06 | 4.125E-03 | 3.540E-03 | 5.854E-04 |
| 2.71 | 1.51 | 0.00 | - | - | 225.24 | 225.24 | 51.96 | 0.110 | 4.583E+06 | 4.084E-03 | 3.452E-03 | 6.319E-04 |
| 3.05 | 1.91 | 0.00 | - | - | 225.24 | 225.24 | 51.96 | 0.124 | 5.156E+06 | 4.085E-03 | 3.378E-03 | 7.070E-04 |
| 3.39 | 2.39 | 0.00 | - | - | 225.24 | 225.24 | 51.96 | 0.138 | 5.729E+06 | 4.130E-03 | 3.313E-03 | 8.170E-04 |
| 3.73 | 2.90 | 0.00 | - | - | 225.24 | 225.24 | 51.96 | 0.152 | 6.302E+06 | 4.149E-03 | 3.256E-03 | 8.930E-04 |
| 4.07 | 3.46 | 0.00 | - | - | 225.24 | 225.24 | 51.96 | 0.165 | 6.874E+06 | 4.156E-03 | 3.205E-03 | 9.510E-04 |
| 4.40 | 4.06 | 0.00 | - | - | 225.24 | 225.24 | 51.96 | 0.179 | 7.447E+06 | 4.164E-03 | 3.160E-03 | 1.004E-03 |
| 4.74 | 4.71 | 0.00 | - | - | 225.24 | 225.24 | 51.96 | 0.193 | 8.020E+06 | 4.157E-03 | 3.118E-03 | 1.039E-03 |
| 5.08 | 5.39 | 0.00 | - | - | 225.24 | 225.24 | 51.96 | 0.207 | 8.593E+06 | 4.145E-03 | 3.081E-03 | 1.064E-03 |
| 5.42 | 6.09 | 0.00 | - | - | 225.24 | 225.24 | 51.96 | 0.220 | 9.166E+06 | 4.118E-03 | 3.046E-03 | 1.072E-03 |
| 5.76 | 6.85 | 0.00 | - | - | 225.24 | 225.24 | 51.96 | 0.234 | 9.739E+06 | 4.103E-03 | 3.014E-03 | 1.089E-03 |
| 6.10 | 7.68 | 0.00 | - | - | 225.24 | 225.24 | 51.96 | 0.248 | 1.031E+07 | 4.105E-03 | 2.984E-03 | 1.121E-03 |
| 6.44 | 8.65 | 0.00 | - | - | 225.24 | 225.24 | 51.96 | 0.262 | 1.088E+07 | 4.148E-03 | 2.956E-03 | 1.192E-03 |
| 6.78 | 9.88 | 0.00 | - | - | 225.24 | 225.24 | 51.96 | 0.276 | 1.146E+07 | 4.276E-03 | 2.930E-03 | 1.345E-03 |
| 7.11 | 11.25 | 0.00 | - | - | 225.24 | 225.24 | 51.96 | 0.289 | 1.203E+07 | 4.419E-03 | 2.906E-03 | 1.513E-03 |
| 7.45 | 12.72 | 0.00 | - | - | 225.24 | 225.24 | 51.96 | 0.303 | 1.260E+07 | 4.551E-03 | 2.883E-03 | 1.668E-03 |
| 7.79 | 14.18 | 0.00 | - | - | 225.24 | 225.24 | 51.96 | 0.317 | 1.318E+07 | 4.642E-03 | 2.861E-03 | 1.781E-03 |
| 8.13 | 15.81 | 0.00 | - | - | 225.24 | 225.24 | 51.96 | 0.331 | 1.375E+07 | 4.753E-03 | 2.841E-03 | 1.912E-03 |
| 8.47 | 17.49 | 0.00 | - | - | 225.24 | 225.24 | 51.96 | 0.344 | 1.432E+07 | 4.846E-03 | 2.821E-03 | 2.025E-03 |
| 8.81 | 19.66 | 0.00 | - | - | 225.24 | 225.24 | 51.96 | 0.358 | 1.489E+07 | 5.035E-03 | 2.803E-03 | 2.233E-03 |
| 9.15 | 22.47 | 0.00 | - | - | 225.24 | 225.24 | 51.96 | 0.372 | 1.547E+07 | 5.338E-03 | 2.785E-03 | 2.553E-03 |
| 9.49 | 25.97 | 0.00 | - | - | 225.24 | 225.24 | 51.96 | 0.386 | 1.604E+07 | 5.735E-03 | 2.768E-03 | 2.967E-03 |
| 9.82 | 30.40 | 0.00 | - | - | 225.24 | 225.24 | 51.96 | 0.400 | 1.661E+07 | 6.259E-03 | 2.752E-03 | 3.507E-03 |
| 10.16 | 34.79 | 0.00 | - | - | 225.24 | 225.24 | 51.96 | 0.413 | 1.719E+07 | 6.693E-03 | 2.737E-03 | 3.957E-03 |
| 10.50 | 39.15 | 0.00 | - | - | 225.24 | 225.24 | 51.96 | 0.427 | 1.776E+07 | 7.054E-03 | 2.722E-03 | 4.332E-03 |
| 10.84 | 44.02 | 0.00 | - | - | 225.24 | 225.24 | 51.96 | 0.441 | 1.833E+07 | 7.444E-03 | 2.707E-03 | 4.737E-03 |
| 11.18 | 48.88 | 0.00 | - | - | 225.24 | 225.24 | 51.96 | 0.455 | 1.890E+07 | 7.772E-03 | 2.694E-03 | 5.078E-03 |
| 11.52 | 53.76 | 0.00 | - | - | 225.24 | 225.24 | 51.96 | 0.469 | 1.948E+07 | 8.053E-03 | 2.681E-03 | 5.372E-03 |

**Table I-2**

**Faired Resistance Data for Model 5415 (Bare Hull)**

41

| Title: | |
|---|---|
| Model Name: | DDG-51 |
| | 5415 |
| Scale Ratio: | 24.824 |
| Ship Displacement: | 8491.2 LT |
| Longitudinal C.G, Ref: | From Mid Ship |
| Longitudinal C.G: | -27.37 ft |
| Frontal Area: | 0.00 sqft |
| Correlation Allowance: | 4.000E-04 |
| Stimulator Penalty: | 0.000E+00 |

| Friction Line: | ITTC |
|---|---|
| Working Fluid: | Salt Water |
| Water Temperature: | 59.0°F |
| Water Density: | 1.991 sl/ft^3 |
| Water Viscosity: | 1.278E-05 ft^2/sec |
| Air Temperature: | 65.0°F |
| Air Density: | 2.351E-03 ft^2/sec |
| Air Viscosity: | 1.608E-04 ft^2/sec |
| Assumed Aero Drag Coef: | 0.000 |

| Laboratory: | NSWC |
|---|---|
| Code Name: | |
| Code Number: | |
| Experimentors: | |
| Test Period: | Shallow Basin |
| Use Form Factor | no |
| Hughes Form Factor | 0.141 |
| Margin: | 0.00% |
| OPC: | |

| Hull Speed Vs (kts) | Total Resistance Rts (lbs) | Effective Horsepower EHP | Delivered Horsepower DHP | Running Trim Ps (deg) | Heave Disp Zs (ft) | Wetted Length Rn WLrs (ft) | Wetted Surface WSAs (sqft) | Froude Number Fn | Reynolds Number Rns | Total Drag Coef Cts | Friction Coef Cfs | Residual Coef Cr |
|---|---|---|---|---|---|---|---|---|---|---|---|---|
| 8.00 | 19,610.6 | 481.8 | | - | - | 465.95 | 32020.0 | 0.110 | 4.923E+08 | 3.375E-03 | 1.675E-03 | 1.301E-03 |
| 9.00 | 25,107.1 | 693.9 | | - | - | 465.95 | 32020.0 | 0.124 | 5.539E+08 | 3.414E-03 | 1.649E-03 | 1.365E-03 |
| 10.00 | 31,378.1 | 963.6 | | - | - | 465.95 | 32020.0 | 0.138 | 6.154E+08 | 3.456E-03 | 1.627E-03 | 1.429E-03 |
| 11.00 | 38,447.8 | 1,298.8 | | - | - | 465.95 | 32020.0 | 0.152 | 6.770E+08 | 3.500E-03 | 1.607E-03 | 1.493E-03 |
| 12.00 | 46,310.8 | 1,706.6 | | - | - | 465.95 | 32020.0 | 0.165 | 7.385E+08 | 3.542E-03 | 1.590E-03 | 1.553E-03 |
| 13.00 | 54,933.0 | 2,193.0 | | - | - | 465.95 | 32020.0 | 0.179 | 8.001E+08 | 3.580E-03 | 1.574E-03 | 1.607E-03 |
| 14.00 | 64,260.7 | 2,762.8 | | - | - | 465.95 | 32020.0 | 0.193 | 8.616E+08 | 3.611E-03 | 1.559E-03 | 1.652E-03 |
| 15.00 | 74,222.9 | 3,419.0 | | - | - | 465.95 | 32020.0 | 0.207 | 9.231E+08 | 3.634E-03 | 1.546E-03 | 1.688E-03 |
| 16.00 | 84,951.0 | 4,174.0 | | - | - | 465.95 | 32020.0 | 0.220 | 9.847E+08 | 3.655E-03 | 1.534E-03 | 1.722E-03 |
| 17.00 | 96,771.4 | 5,052.0 | | - | - | 465.95 | 32020.0 | 0.234 | 1.046E+09 | 3.688E-03 | 1.522E-03 | 1.766E-03 |
| 18.00 | 110,160.3 | 6,089.3 | | - | - | 465.95 | 32020.0 | 0.248 | 1.108E+09 | 3.745E-03 | 1.511E-03 | 1.834E-03 |
| 19.00 | 125,739.4 | 7,336.5 | | - | - | 465.95 | 32020.0 | 0.262 | 1.169E+09 | 3.837E-03 | 1.501E-03 | 1.935E-03 |
| 20.00 | 143,522.5 | 8,814.9 | | - | - | 465.95 | 32020.0 | 0.276 | 1.231E+09 | 3.952E-03 | 1.492E-03 | 2.060E-03 |
| 21.00 | 162,744.0 | 10,495.1 | | - | - | 465.95 | 32020.0 | 0.289 | 1.292E+09 | 4.065E-03 | 1.483E-03 | 2.182E-03 |
| 22.00 | 182,262.0 | 12,313.6 | | - | - | 465.95 | 32020.0 | 0.303 | 1.354E+09 | 4.148E-03 | 1.475E-03 | 2.273E-03 |
| 23.00 | 200,927.0 | 14,191.7 | | - | - | 465.95 | 32020.0 | 0.317 | 1.416E+09 | 4.184E-03 | 1.467E-03 | 2.317E-03 |
| 24.00 | 220,064.6 | 16,219.1 | | - | - | 465.95 | 32020.0 | 0.331 | 1.477E+09 | 4.208E-03 | 1.459E-03 | 2.349E-03 |
| 25.00 | 242,629.8 | 18,627.4 | | - | - | 465.95 | 32020.0 | 0.344 | 1.539E+09 | 4.276E-03 | 1.452E-03 | 2.424E-03 |
| 26.00 | 272,559.8 | 21,762.1 | | - | - | 465.95 | 32020.0 | 0.358 | 1.600E+09 | 4.441E-03 | 1.445E-03 | 2.596E-03 |
| 27.00 | 314,140.4 | 26,046.9 | | - | - | 465.95 | 32020.0 | 0.372 | 1.662E+09 | 4.747E-03 | 1.439E-03 | 2.908E-03 |
| 28.00 | 368,507.9 | 31,686.2 | | - | - | 465.95 | 32020.0 | 0.386 | 1.723E+09 | 5.178E-03 | 1.432E-03 | 3.345E-03 |
| 29.00 | 433,011.4 | 38,562.5 | | - | - | 465.95 | 32020.0 | 0.400 | 1.785E+09 | 5.671E-03 | 1.426E-03 | 3.845E-03 |
| 30.00 | 502,194.2 | 46,267.4 | | - | - | 465.95 | 32020.0 | 0.413 | 1.846E+09 | 6.146E-03 | 1.420E-03 | 4.326E-03 |
| 31.00 | 570,294.5 | 54,289.0 | | - | - | 465.95 | 32020.0 | 0.427 | 1.908E+09 | 6.537E-03 | 1.415E-03 | 4.722E-03 |
| 32.00 | 638,912.3 | 62,784.5 | | - | - | 465.95 | 32020.0 | 0.441 | 1.969E+09 | 6.873E-03 | 1.410E-03 | 5.063E-03 |

NOTE: These values are based upon the bare hull resistance using the OPC at 32 knots based upon sea trials

**Table I-3**

**Resistance Data for Bare Hull Model 5415 Expanded To Full Scale**

41

(THIS PAGE INTENTIONALLY LEFT BLANK)

# APPENDIX II

# DDG51/VMP COMPARISON

To:     F. Peterson (5400)
From:   G. Karafiath (5200), D. Cusanelli (5200)

Subj:   DDG 51 COMPARISON TO VAMP

Encl:   (1) Detailed powering performance of DDG 51 for comparison to VAMP

1) We have looked at the DDG 51 performance to determine the case for comparison to VAMP. The effect of the forebody difference between the VAMP model and the fleet DDG 51 hullform is estimated to be less than 2 % on resistance. Thus, the comparison of the VAMP model results to the fleet DDG 51 results is mostly a comparison of propulsor design differences.

2) DDG 51 fleet performance is represented by a powering prediction at CA=0.00015 as determined by ship/model correlation experiments. All VAMP tests were conducted at CA=0.0004. It is our recommendation that the VAMP be compared to the DDG 51 at equivalent CA=0.0004, at the equivalent 8500 ton displacement, as shown below:

|  | DDG 51 8740 tons CA=0.00015 [in McMahon presentation] | DDG 51 8500 tons CA=0.0004 |
|---|---|---|
| VS (knots) | SHP (hP) | SHP (hP) |
| 12 | 2200 | 2634 |
| 20 | 12450 | 13363 |
| 28 | 49420 | 49862 |

3) With regard to the VAMP presentation (McMahon), we are concerned that there is no presentation of flow rates as a function of speed, or pump efficiency as a function of speed. Open propeller efficiency tends to vary as a function of speed, and we would expect the pump efficiency to also do so.

Dominic S. Cusanelli
Gabor Karafiath

A hard copy of this memorandum will also be forwarded.

The forebody of the modified VAMP model, 5484-1, is identical to that of the preliminary DDG hull design as represented by Models 5415 (wood) and 5482 (fiberglass). Therefore, the most accurate comparison between the VAMP model and the

DDG with similar forebody, would be an estimate of the previous Model 5415 powering at 8500 tons with the ATD propellers. There exists no previous Model 5415 tests conducted with ATD propellers. If you feel this comparison is warranted, a greater time frame is necessary to adjust the Model 5415 powering data to the aforementioned conditions.

The present DDG 51 fleet design hull form is represented by Model 5513. Model 5513 is a re-manufactured fiberglass version of the contract design DDG 51 Model 5422 (wood). Model 5513 includes several modifications to the hull and appendages to insure that the model is as closely representative of the full scale "as built" DDG 51 Class Flight I hullform as possible. At 8500 tons, the preliminary DDG 51 design Models 5415 & 5484 and the fleet design Model 5513 have the following characteristics:

Table 1

| | Beam (ft) | Draft (ft) | Wetted Surface (ft2) |
|---|---|---|---|
| Preliminary DDG 51 | 61.9 | 20.22 | 34438 |
| Fleet DDG 51 | 59.0 | 20.81 | 34146 |

Referring back through many reports, the following resistance comparisons can be made at the speeds of interest for the VAMP data. All data are compared at CA = 0.0004.

Table 2a
Bare Hull Resistance, EHP (hP)

| VS (knots) | Preliminary DDG 51 | Fleet DDG 51 | Fleet/Preliminary |
|---|---|---|---|
| 12 | 1410 | 1415 | 1.0 |
| 20 | 7190 | 7070 | 0.98 |
| 28 | 29250 | 28630 | 0.98 |

Table 2b
Fully Appended Resistance, EHP (hP)

| VS (knots) | Preliminary DDG 51 | Fleet DDG 51 | Fleet/Preliminary |
|---|---|---|---|
| 12 | 1750 | 1820 | 1.04 |
| 20 | 8970 | 9180 | 1.02 |
| 28 | 33760 | 33490 | 0.99 |

From the above two tables, we can conclude that the effect of the changes in forebody, draft, beam, etc., between the DDG 51 preliminary design and fleet design hullforms, is within roughly +/- 2 percent, at the higher speeds. Therefore, a comparison of the preliminary design DDG 51 forebody, as tested in the VAMP model, to the fleet DDG 51 hullform data, can be considered to be representative of mostly the propulsor / appendage differences.

No previous fleet design Model 5513 tests were conducted at the conditions utilized in the VAMP analysis. Therefore, adjustments were made to existing Model 5513 data to estimate the following summary, Table 3, of DDG 51 fleet performances comparable to

the conditions of the VAMP analysis. Complete powering data are provided as Tables 4 and 5 below.

Table 3

| VS (knots) | CA = 0.00015 | CA = 0.0004 |
|---|---|---|
| 12 | 2448 | 2634 |
| 20 | 12475 | 13363 |
| 28 | 47236 | 49862 |

The ship/model correlation between fleet design Model 5513 and the BARRY (DDG 52) trials with ATD propellers, indicated that the at sea performance of the DDG 51 Class is best represented by a correlation allowance of CA=0.00015, as provided in Table 4. Your requirement, for the most accurate representation of the performance of the present DDG 51, at your specified 8500 ton displacement, would be best satisfied by Table 4. However, it is our opinion, that the comparison between the VAMP and the DDG 51 fleet design, should be at identical values of CA = 0.0004, as provided in Table 5.

According to J. Hoyt, the "DDG 51" data in the VAMP presentation put together by J. McMahon, represented the DDG 51 fleet design Model 5513 at 8740 tons, at a correlation allowance of CA = 0.00015. The data was from report 1269-02, Table B10, which was presented at only the trials speeds, and had been adjusted to eliminate the full scale effects of wind. The present suggested values of power differ from the previous values because of: CA = 0.0004, displacement of 8500 tons, and no wind correction.

With regard to the aforementioned VAMP presentation, we are concerned that there is no presentation of flow rates as a function of speed, or pump efficiency as a function of speed. Open propeller efficiency tends to vary as a function of speed, and we would expect the pump efficiency to also do so.

## Table 4. Estimate: DDG51 Model 5513 @8500t ATDprop CA=0.00015
Represents full scale trials performance adjusted for VAMP model test displacement

```
SHIP LENGTH           467.0 FEET   ( 142.3 METERS)
SHIP DISPLACEMENT     8500. TONS   ( 8638. METRIC TONS)
SHIP WETTED SURFACE   34146. SQFT  ( 3172. SQ METERS)
CORRELATION ALLOWANCE .00015       ITTC FRICTION USED
```

| | SHIP SPEED | | RESIDUARY RES.COEF. | EFFECTIVE POWER- PE | | DELIVERED POWER- PD | | PROPELLER REV. PER | |
|---|---|---|---|---|---|---|---|---|---|
| I | (KTS) | (M/S) | (CR*1000) | (HP) | (kW) | (HP) | (kW) | MINUTE | I |
| I | 10.0 | 5.14 | 1.441 | 956.0 | 712.9 | 1382.1 | 1030.7 | 44.1 | I |
| I | 11.0 | 5.66 | 1.505 | 1290.0 | 962.0 | 1864.4 | 1390.3 | 48.4 | I |
| I | 12.0 | 6.17 | 1.560 | 1694.0 | 1263.2 | 2448.1 | 1825.5 | 52.8 | I |
| I | 13.0 | 6.69 | 1.602 | 2171.0 | 1618.9 | 3137.2 | 2339.4 | 57.2 | I |
| I | 14.0 | 7.20 | 1.633 | 2725.0 | 2032.0 | 3937.2 | 2936.0 | 61.7 | I |
| I | 15.0 | 7.72 | 1.654 | 3359.0 | 2504.8 | 4857.7 | 3622.3 | 66.2 | I |
| I | 16.0 | 8.23 | 1.685 | 4099.0 | 3056.6 | 5927.6 | 4420.2 | 70.7 | I |
| I | 17.0 | 8.75 | 1.731 | 4967.0 | 3703.9 | 7197.4 | 5367.1 | 75.4 | I |
| I | 18.0 | 9.26 | 1.796 | 5990.0 | 4466.7 | 8681.4 | 6473.7 | 80.1 | I |
| I | 19.0 | 9.77 | 1.865 | 7165.0 | 5342.9 | 10407.0 | 7760.5 | 84.9 | I |
| I | 20.0 | 10.29 | 1.970 | 8584.0 | 6401.1 | 12475.9 | 9303.3 | 89.7 | I |
| I | 21.0 | 10.80 | 2.125 | 10340.0 | 7710.5 | 15066.0 | 11234.7 | 94.6 | I |
| I | 22.0 | 11.32 | 2.247 | 12249.0 | 9134.1 | 17871.8 | 13327.0 | 99.5 | I |
| I | 23.0 | 11.83 | 2.292 | 14127.0 | 10534.5 | 20677.1 | 15418.9 | 104.4 | I |
| I | 24.0 | 12.35 | 2.332 | 16186.0 | 12069.9 | 23742.6 | 17704.9 | 109.2 | I |
| I | 25.0 | 12.86 | 2.398 | 18566.0 | 13844.7 | 27317.1 | 20370.4 | 114.4 | I |
| I | 26.0 | 13.38 | 2.535 | 21565.0 | 16081.0 | 31833.7 | 23738.4 | 119.8 | I |
| I | 27.0 | 13.89 | 2.835 | 25870.0 | 19291.3 | 38231.5 | 28509.2 | 125.7 | I |
| I | 28.0 | 14.40 | 3.303 | 31861.0 | 23758.7 | 47236.6 | 35224.3 | 132.3 | I |
| I | 29.0 | 14.92 | 3.744 | 38551.0 | 28747.5 | 57297.0 | 42726.3 | 139.7 | I |
| I | 30.0 | 15.43 | 4.195 | 46250.0 | 34488.6 | 68968.2 | 51429.6 | 147.8 | I |
| I | 31.0 | 15.95 | 4.648 | 54987.0 | 41003.8 | 82290.1 | 61363.7 | 156.0 | I |
| I | 32.0 | 16.46 | 4.942 | 63288.0 | 47193.9 | 95016.8 | 70854.0 | 162.6 | I |
| I | 33.0 | 16.98 | 5.146 | 71537.0 | 53345.1 | 107810.5 | 80394.3 | 167.6 | I |

| | SHIP SPEED | EFFICIENCIES (ETA) | | | | | THRUST DEDUCTION AND WAKE FACTORS | | | ADVANCE COEF. | |
|---|---|---|---|---|---|---|---|---|---|---|---|
| I | (KTS) | ETAD | ETAO | ETAH | ETAR | ETAB | 1-THDF | 1-WFTT | 1-WFTQ | ADVC | I |
| I | 10.0 | 0.690 | 0.760 | 0.980 | 0.930 | 0.705 | 0.985 | 1.005 | 0.980 | 1.360 | I |
| I | 11.0 | 0.690 | 0.760 | 0.980 | 0.930 | 0.705 | 0.975 | 1.000 | 0.975 | 1.350 | I |
| I | 12.0 | 0.690 | 0.760 | 0.980 | 0.930 | 0.710 | 0.970 | 0.995 | 0.970 | 1.345 | I |
| I | 13.0 | 0.690 | 0.760 | 0.975 | 0.930 | 0.710 | 0.965 | 0.990 | 0.965 | 1.340 | I |
| I | 14.0 | 0.690 | 0.760 | 0.970 | 0.935 | 0.710 | 0.965 | 0.990 | 0.970 | 1.340 | I |
| I | 15.0 | 0.690 | 0.760 | 0.965 | 0.940 | 0.715 | 0.960 | 0.990 | 0.970 | 1.340 | I |
| I | 16.0 | 0.690 | 0.760 | 0.965 | 0.945 | 0.720 | 0.955 | 0.990 | 0.970 | 1.335 | I |
| I | 17.0 | 0.690 | 0.760 | 0.960 | 0.945 | 0.720 | 0.955 | 0.995 | 0.975 | 1.335 | I |
| I | 18.0 | 0.690 | 0.760 | 0.955 | 0.950 | 0.720 | 0.950 | 0.995 | 0.975 | 1.330 | I |
| I | 19.0 | 0.690 | 0.760 | 0.955 | 0.950 | 0.725 | 0.950 | 0.995 | 0.975 | 1.325 | I |
| I | 20.0 | 0.690 | 0.760 | 0.955 | 0.950 | 0.720 | 0.945 | 0.995 | 0.975 | 1.320 | I |
| I | 21.0 | 0.685 | 0.760 | 0.955 | 0.945 | 0.720 | 0.945 | 0.990 | 0.965 | 1.305 | I |
| I | 22.0 | 0.685 | 0.760 | 0.960 | 0.945 | 0.715 | 0.945 | 0.985 | 0.960 | 1.300 | I |
| I | 23.0 | 0.685 | 0.760 | 0.955 | 0.945 | 0.715 | 0.945 | 0.990 | 0.965 | 1.295 | I |
| I | 24.0 | 0.680 | 0.760 | 0.955 | 0.945 | 0.715 | 0.945 | 0.990 | 0.965 | 1.295 | I |
| I | 25.0 | 0.680 | 0.760 | 0.950 | 0.945 | 0.715 | 0.945 | 0.995 | 0.970 | 1.295 | I |
| I | 26.0 | 0.675 | 0.755 | 0.950 | 0.940 | 0.715 | 0.945 | 0.995 | 0.970 | 1.290 | I |
| I | 27.0 | 0.675 | 0.755 | 0.955 | 0.940 | 0.710 | 0.945 | 0.990 | 0.960 | 1.270 | I |
| I | 28.0 | 0.675 | 0.750 | 0.965 | 0.935 | 0.700 | 0.950 | 0.980 | 0.945 | 1.240 | I |
| I | 29.0 | 0.675 | 0.745 | 0.965 | 0.935 | 0.695 | 0.950 | 0.985 | 0.945 | 1.215 | I |
| I | 30.0 | 0.670 | 0.740 | 0.960 | 0.945 | 0.695 | 0.955 | 0.995 | 0.960 | 1.200 | I |
| I | 31.0 | 0.670 | 0.735 | 0.955 | 0.950 | 0.700 | 0.960 | 1.000 | 0.970 | 1.185 | I |
| I | 32.0 | 0.665 | 0.730 | 0.960 | 0.950 | 0.695 | 0.960 | 1.000 | 0.965 | 1.175 | I |
| I | 33.0 | 0.665 | 0.725 | 0.980 | 0.935 | 0.680 | 0.965 | 0.990 | 0.945 | 1.160 | I |

## Table 5. Estimate: DDG51 Model 5513 @8500t ATDprop CA=0.0004
Represents full scale trials performance adjusted for VAMP model displacement and CA

```
SHIP LENGTH            467.0 FEET   ( 142.3 METERS)
SHIP DISPLACEMENT      8500. TONS   ( 8638. METRIC TONS)
SHIP WETTED SURFACE   34146. SQFT   ( 3172. SQ METERS)
CORRELATION ALLOWANCE  .00040       ITTC FRICTION USED
```

| I | SHIP SPEED | | RESIDUARY RES.COEF. | EFFECTIVE POWER- PE | | DELIVERED POWER- PD | | PROPELLER REV. PER | I |
|---|---|---|---|---|---|---|---|---|---|
| I | (KTS) | (M/S) | (CR*1000) | (HP) | (kW) | (HP) | (kW) | MINUTE | I |
| I | 10.0 | 5.14 | 1.441 | 1030.4 | 768.3 | 1488.6 | 1110.0 | 44.6 | I |
| I | 11.0 | 5.66 | 1.505 | 1388.9 | 1035.7 | 2007.0 | 1496.6 | 49.0 | I |
| I | 12.0 | 6.17 | 1.560 | 1822.4 | 1359.0 | 2634.1 | 1964.3 | 53.4 | I |
| I | 13.0 | 6.69 | 1.602 | 2334.0 | 1740.5 | 3374.3 | 2516.2 | 57.9 | I |
| I | 14.0 | 7.20 | 1.633 | 2928.5 | 2183.8 | 4233.7 | 3157.1 | 62.5 | I |
| I | 15.0 | 7.72 | 1.654 | 3609.6 | 2691.7 | 5223.4 | 3895.1 | 67.0 | I |
| I | 16.0 | 8.23 | 1.685 | 4403.4 | 3283.6 | 6372.7 | 4752.1 | 71.6 | I |
| I | 17.0 | 8.75 | 1.731 | 5332.1 | 3976.1 | 7733.2 | 5766.7 | 76.4 | I |
| I | 18.0 | 9.26 | 1.796 | 6423.5 | 4790.0 | 9320.5 | 6950.3 | 81.1 | I |
| I | 19.0 | 9.77 | 1.865 | 7674.8 | 5723.1 | 11162.5 | 8323.9 | 85.9 | I |
| I | 20.0 | 10.29 | 1.970 | 9178.7 | 6844.6 | 13363.4 | 9965.1 | 90.8 | I |
| I | 21.0 | 10.80 | 2.125 | 11027.5 | 8223.2 | 16104.7 | 12009.3 | 95.7 | I |
| I | 22.0 | 11.32 | 2.247 | 13038.5 | 9722.8 | 19074.3 | 14223.7 | 100.7 | I |
| I | 23.0 | 11.83 | 2.292 | 15032.4 | 11209.6 | 22061.4 | 16451.1 | 105.6 | I |
| I | 24.0 | 12.35 | 2.332 | 17212.9 | 12835.6 | 25317.2 | 18879.0 | 110.5 | I |
| I | 25.0 | 12.86 | 2.398 | 19728.4 | 14711.4 | 29106.0 | 21704.3 | 115.8 | I |
| I | 26.0 | 13.38 | 2.535 | 22871.2 | 17055.1 | 33861.1 | 25250.2 | 121.2 | I |
| I | 27.0 | 13.89 | 2.835 | 27328.9 | 20379.2 | 40529.8 | 30223.1 | 127.1 | I |
| I | 28.0 | 14.40 | 3.303 | 33490.5 | 24973.9 | 49862.6 | 37182.6 | 133.8 | I |
| I | 29.0 | 14.92 | 3.744 | 40360.1 | 30096.5 | 60256.7 | 44933.4 | 141.2 | I |
| I | 30.0 | 15.43 | 4.195 | 48252.2 | 35981.6 | 72284.7 | 53902.7 | 149.3 | I |
| I | 31.0 | 15.95 | 4.648 | 57200.1 | 42654.1 | 86000.6 | 64130.6 | 157.5 | I |
| I | 32.0 | 16.46 | 4.942 | 65726.0 | 49011.9 | 99145.2 | 73932.5 | 164.1 | I |
| I | 33.0 | 16.98 | 5.146 | 74205.4 | 55334.9 | 112380.0 | 83801.8 | 169.2 | I |

| I | SHIP SPEED | EFFICIENCIES (ETA) | | | | | THRUST DEDUCTION AND WAKE FACTORS | | | ADVANCE COEF. | I |
|---|---|---|---|---|---|---|---|---|---|---|---|
| I | (KTS) | ETAD | ETAO | ETAH | ETAR | ETAB | 1-THDF | 1-WFTT | 1-WFTQ | ADVC | I |
| I | 10.0 | 0.690 | 0.760 | 0.980 | 0.930 | 0.710 | 0.985 | 1.005 | 0.980 | 1.340 | I |
| I | 11.0 | 0.690 | 0.760 | 0.980 | 0.930 | 0.710 | 0.975 | 1.000 | 0.975 | 1.335 | I |
| I | 12.0 | 0.690 | 0.760 | 0.980 | 0.930 | 0.710 | 0.970 | 0.995 | 0.965 | 1.330 | I |
| I | 13.0 | 0.690 | 0.760 | 0.975 | 0.930 | 0.710 | 0.965 | 0.990 | 0.965 | 1.325 | I |
| I | 14.0 | 0.690 | 0.760 | 0.970 | 0.935 | 0.710 | 0.965 | 0.990 | 0.965 | 1.325 | I |
| I | 15.0 | 0.690 | 0.760 | 0.965 | 0.940 | 0.715 | 0.960 | 0.990 | 0.970 | 1.320 | I |
| I | 16.0 | 0.690 | 0.760 | 0.965 | 0.945 | 0.720 | 0.955 | 0.990 | 0.970 | 1.320 | I |
| I | 17.0 | 0.690 | 0.760 | 0.960 | 0.945 | 0.720 | 0.955 | 0.995 | 0.975 | 1.320 | I |
| I | 18.0 | 0.690 | 0.760 | 0.955 | 0.950 | 0.720 | 0.950 | 0.995 | 0.970 | 1.315 | I |
| I | 19.0 | 0.690 | 0.760 | 0.955 | 0.950 | 0.720 | 0.950 | 0.995 | 0.975 | 1.310 | I |
| I | 20.0 | 0.685 | 0.760 | 0.955 | 0.950 | 0.720 | 0.945 | 0.995 | 0.970 | 1.305 | I |
| I | 21.0 | 0.685 | 0.760 | 0.955 | 0.945 | 0.715 | 0.945 | 0.990 | 0.965 | 1.290 | I |
| I | 22.0 | 0.685 | 0.755 | 0.960 | 0.945 | 0.715 | 0.945 | 0.985 | 0.960 | 1.280 | I |
| I | 23.0 | 0.680 | 0.755 | 0.955 | 0.945 | 0.715 | 0.945 | 0.990 | 0.960 | 1.280 | I |
| I | 24.0 | 0.680 | 0.755 | 0.955 | 0.945 | 0.715 | 0.945 | 0.990 | 0.965 | 1.280 | I |
| I | 25.0 | 0.680 | 0.755 | 0.950 | 0.945 | 0.715 | 0.945 | 0.995 | 0.970 | 1.280 | I |
| I | 26.0 | 0.675 | 0.755 | 0.950 | 0.940 | 0.710 | 0.945 | 0.995 | 0.970 | 1.275 | I |
| I | 27.0 | 0.675 | 0.750 | 0.955 | 0.940 | 0.705 | 0.945 | 0.990 | 0.960 | 1.255 | I |
| I | 28.0 | 0.670 | 0.745 | 0.965 | 0.935 | 0.695 | 0.950 | 0.980 | 0.945 | 1.225 | I |
| I | 29.0 | 0.670 | 0.740 | 0.965 | 0.935 | 0.690 | 0.950 | 0.985 | 0.945 | 1.205 | I |
| I | 30.0 | 0.670 | 0.735 | 0.960 | 0.945 | 0.695 | 0.955 | 0.995 | 0.960 | 1.190 | I |
| I | 31.0 | 0.665 | 0.730 | 0.955 | 0.950 | 0.695 | 0.960 | 1.000 | 0.970 | 1.175 | I |
| I | 32.0 | 0.665 | 0.725 | 0.960 | 0.950 | 0.690 | 0.960 | 1.000 | 0.965 | 1.160 | I |
| I | 33.0 | 0.660 | 0.720 | 0.980 | 0.935 | 0.675 | 0.965 | 0.990 | 0.940 | 1.150 | I |

# APPENDIX III

# RESISTANCE DATA FOR HULL MODEL 5482-1

| Title: | Waterjet Concept | Friction Line: | ITTC | Labotatory: | NSWC |
|---|---|---|---|---|---|
| Model Name: | 5482-1 | Working Fluid: | Fresh Water | Code Name: | Seakeeping |
| Model Weight: | 1212.00 lbs | Water Temperature: | 66.0°F | Code Number: | Code 5500 |
| Longitudinal C.G, Ref: | From Mid Ship | Water Density: | 1.937 sl/ft^3 | Experimentors: | Burke, Hickok, Hoyt III |
| Longitudinal C.G: | -13.23 in | Water Viscosity: | 1.110E-05 ft^2/sec | Facility: | Shallow Basin |
| Frontal Area: | 0.00 sqin | Air Temperature: | 74.0°F | Carriage: | Carriage 1 |
| Stimulator: | Studs | Air Density: | 2.311E-03 ft^2/sec | Test Period: | January 1997 |
| Stimulator Penalty: | 0.000E+00 | Air Viscosity: | 1.657E-04 ft^2/sec | Sponsor: | ONR |
| Correlation Allowance: | 4.000E-04 | Assumed Aero Drag Coef: | 0.000 | Job Order Number: | 1-5060-753-20 |

| Hull Speed Vm (fps) | Total Resistance Rtm (lbs) | Areo Resistance Ram (lbs) | Running Trim Pm (deg) | Heave Disp Zm (in) | Wetted Length Fn WLfm (in) | Wetted Length Rn WLrm (in) | Wetted Surface WSAm (sqft) | Froude Number Fn | Reynolds Number Rnm | Total Drag Coef Ctm | Friction Coef Cfm | Residual Coef Cr |
|---|---|---|---|---|---|---|---|---|---|---|---|---|
| 2.67 | 1.61 | 0.00 | -0.01 | -0.05 | 225.24 | 225.24 | 51.96 | 0.108 | 4.509E+06 | 4.511E-03 | 3.462E-03 | 1.049E-03 |
| 3.35 | 2.43 | 0.00 | 0.01 | -0.08 | 225.24 | 225.24 | 51.96 | 0.136 | 5.666E+06 | 4.295E-03 | 3.320E-03 | 9.756E-04 |
| 4.03 | 3.61 | 0.00 | -0.02 | -0.14 | 225.24 | 225.24 | 51.96 | 0.164 | 6.820E+06 | 4.410E-03 | 3.210E-03 | 1.200E-03 |
| 4.70 | 4.97 | 0.00 | 0.00 | -0.20 | 225.24 | 225.24 | 51.96 | 0.191 | 7.944E+06 | 4.477E-03 | 3.124E-03 | 1.353E-03 |
| 5.36 | 6.42 | 0.00 | -0.03 | -0.27 | 225.24 | 225.24 | 51.96 | 0.218 | 9.064E+06 | 4.440E-03 | 3.052E-03 | 1.388E-03 |
| 6.05 | 8.45 | 0.00 | 0.00 | -0.35 | 225.24 | 225.24 | 51.96 | 0.246 | 1.022E+07 | 4.596E-03 | 2.989E-03 | 1.607E-03 |
| 6.73 | 11.09 | 0.00 | -0.06 | -0.43 | 225.24 | 225.24 | 51.96 | 0.274 | 1.138E+07 | 4.869E-03 | 2.934E-03 | 1.935E-03 |
| 6.73 | 11.09 | 0.00 | -0.04 | -0.44 | 225.24 | 225.24 | 51.96 | 0.274 | 1.138E+07 | 4.865E-03 | 2.934E-03 | 1.931E-03 |
| 6.74 | 11.10 | 0.00 | -0.04 | -0.42 | 225.24 | 225.24 | 51.96 | 0.274 | 1.139E+07 | 4.861E-03 | 2.933E-03 | 1.928E-03 |
| 7.43 | 14.27 | 0.00 | 0.00 | -0.53 | 225.24 | 225.24 | 51.96 | 0.302 | 1.257E+07 | 5.132E-03 | 2.884E-03 | 2.247E-03 |
| 8.08 | 17.57 | 0.00 | -0.06 | -0.63 | 225.24 | 225.24 | 51.96 | 0.329 | 1.367E+07 | 5.346E-03 | 2.844E-03 | 2.502E-03 |
| 8.08 | 17.56 | 0.00 | -0.03 | -0.64 | 225.24 | 225.24 | 51.96 | 0.329 | 1.367E+07 | 5.338E-03 | 2.843E-03 | 2.495E-03 |
| 8.09 | 17.53 | 0.00 | -0.04 | -0.60 | 225.24 | 225.24 | 51.96 | 0.329 | 1.369E+07 | 5.320E-03 | 2.843E-03 | 2.477E-03 |
| 8.76 | 21.93 | 0.00 | -0.02 | -0.71 | 225.24 | 225.24 | 51.96 | 0.356 | 1.481E+07 | 5.679E-03 | 2.805E-03 | 2.874E-03 |
| 9.43 | 27.80 | 0.00 | 0.20 | -0.78 | 225.24 | 225.24 | 51.96 | 0.383 | 1.594E+07 | 6.217E-03 | 2.771E-03 | 3.446E-03 |
| 9.44 | 27.86 | 0.00 | 0.20 | -0.78 | 225.24 | 225.24 | 51.96 | 0.384 | 1.596E+07 | 6.217E-03 | 2.770E-03 | 3.446E-03 |
| 10.11 | 37.33 | 0.00 | 0.50 | -0.78 | 225.24 | 225.24 | 51.96 | 0.411 | 1.709E+07 | 7.258E-03 | 2.739E-03 | 4.519E-03 |
| 10.76 | 45.64 | 0.00 | 0.88 | -0.72 | 225.24 | 225.24 | 51.96 | 0.438 | 1.819E+07 | 7.836E-03 | 2.711E-03 | 5.125E-03 |
| 10.83 | 47.14 | 0.00 | 0.92 | -0.72 | 225.24 | 225.24 | 51.96 | 0.441 | 1.831E+07 | 7.987E-03 | 2.708E-03 | 5.279E-03 |

**Table III-1**

**Raw Resistance Data for Bare Hull Model 5482-1**

| | | |
|---|---|---|
| **Title:** Waterjet Concept | **Friction Line:** ITTC | **Labotatory:** NSWC |
| **Model Name:** 5482-1 | **Working Fluid:** Fresh Water | **Code Name:** Seakeeping |
| **Model Weight:** 1212.00 lbs | **Water Temperature:** 66.0°F | **Code Number:** Code 5500 |
| **Longitudinal C.G, Ref.:** From Mid Ship | **Water Density:** 1.937 sl/ft^3 | **Experimenters:** Burke, Hickok, Hoyt III |
| **Longitudinal C.G:** -13.23 in | **Water Viscosity:** 1.110E-05 ft^2/sec | **Facility:** Shallow Basin |
| **Frontal Area:** 0.00 sqin | **Air Temperature:** 74.0°F | **Carriage:** Carriage 1 |
| **Stimulator:** Studs | **Air Density:** 2.311E-03 ft^2/sec | **Test Period:** January 1997 |
| **Stimulator Penalty:** 0.000E+00 | **Air Viscosity:** 1.657E-04 ft^2/sec | **Sponsor:** ONR |
| **Correlation Allowance:** 4.000E-04 | **Assumed Aero Drag Coef:** 0.000 | **Job Order Number:** 1-5060-753-20 |

| Hull Speed $V_m$ (fps) | Total Resistance $R_{tm}$ (lbs) | Areo Resistance $R_{am}$ (lbs) | Running Trim $P_m$ (deg) | Heave Disp $Z_m$ (in) | Wetted Length Fn $WL_{fm}$ (in) | Wetted Length Rn $WL_{rm}$ (in) | Wetted Surface $WSA_m$ (sqft) | Froude Number $F_n$ | Reynolds Number $R_{nm}$ | Total Drag Coef $C_{tm}$ | Friction Coef $C_{fm}$ | Residual Coef $C_r$ |
|---|---|---|---|---|---|---|---|---|---|---|---|---|
| 0.00 | 0.00 | 0.00 | 0.00 | 0.00 | 225.24 | 225.24 | 51.96 | 0.000 | 0.000E+00 | - | - | - |
| 0.34 | 0.14 | 0.00 | 0.00 | 0.00 | 225.24 | 225.24 | 51.96 | 0.014 | 5.729E+05 | 6.576E-03 | 5.311E-03 | 1.265E-03 |
| 0.68 | 0.28 | 0.00 | 0.00 | 0.00 | 225.24 | 225.24 | 51.96 | 0.028 | 1.146E+06 | 5.637E-03 | 4.552E-03 | 1.085E-03 |
| 1.02 | 0.44 | 0.00 | -0.01 | -0.01 | 225.24 | 225.24 | 51.96 | 0.041 | 1.719E+06 | 5.179E-03 | 4.181E-03 | 9.978E-04 |
| 1.36 | 0.62 | 0.00 | -0.01 | -0.01 | 225.24 | 225.24 | 51.96 | 0.055 | 2.291E+06 | 4.891E-03 | 3.945E-03 | 9.454E-04 |
| 1.69 | 0.82 | 0.00 | -0.01 | -0.02 | 225.24 | 225.24 | 51.96 | 0.069 | 2.864E+06 | 4.689E-03 | 3.775E-03 | 9.131E-04 |
| 2.03 | 1.06 | 0.00 | -0.01 | -0.03 | 225.24 | 225.24 | 51.96 | 0.083 | 3.437E+06 | 4.542E-03 | 3.645E-03 | 8.967E-04 |
| 2.37 | 1.33 | 0.00 | -0.01 | -0.04 | 225.24 | 225.24 | 51.96 | 0.096 | 4.010E+06 | 4.436E-03 | 3.540E-03 | 8.960E-04 |
| 2.71 | 1.65 | 0.00 | -0.01 | -0.05 | 225.24 | 225.24 | 51.96 | 0.110 | 4.583E+06 | 4.365E-03 | 3.452E-03 | 9.124E-04 |
| 3.05 | 2.03 | 0.00 | -0.02 | -0.06 | 225.24 | 225.24 | 51.96 | 0.124 | 5.156E+06 | 4.332E-03 | 3.378E-03 | 9.549E-04 |
| 3.39 | 2.49 | 0.00 | -0.02 | -0.08 | 225.24 | 225.24 | 51.96 | 0.138 | 5.729E+06 | 4.306E-03 | 3.313E-03 | 9.930E-04 |
| 3.73 | 3.04 | 0.00 | -0.02 | -0.11 | 225.24 | 225.24 | 51.96 | 0.152 | 6.302E+06 | 4.357E-03 | 3.256E-03 | 1.101E-03 |
| 4.07 | 3.68 | 0.00 | -0.02 | -0.13 | 225.24 | 225.24 | 51.96 | 0.165 | 6.874E+06 | 4.423E-03 | 3.205E-03 | 1.218E-03 |
| 4.40 | 4.36 | 0.00 | -0.02 | -0.16 | 225.24 | 225.24 | 51.96 | 0.179 | 7.447E+06 | 4.466E-03 | 3.160E-03 | 1.306E-03 |
| 4.74 | 5.06 | 0.00 | -0.02 | -0.19 | 225.24 | 225.24 | 51.96 | 0.193 | 8.020E+06 | 4.468E-03 | 3.118E-03 | 1.350E-03 |
| 5.08 | 5.77 | 0.00 | -0.03 | -0.23 | 225.24 | 225.24 | 51.96 | 0.207 | 8.593E+06 | 4.443E-03 | 3.081E-03 | 1.363E-03 |
| 5.42 | 6.57 | 0.00 | -0.03 | -0.26 | 225.24 | 225.24 | 51.96 | 0.220 | 9.166E+06 | 4.445E-03 | 3.046E-03 | 1.399E-03 |
| 5.76 | 7.51 | 0.00 | -0.03 | -0.30 | 225.24 | 225.24 | 51.96 | 0.234 | 9.739E+06 | 4.501E-03 | 3.014E-03 | 1.487E-03 |
| 6.10 | 8.62 | 0.00 | -0.04 | -0.33 | 225.24 | 225.24 | 51.96 | 0.248 | 1.031E+07 | 4.605E-03 | 2.984E-03 | 1.620E-03 |
| 6.44 | 9.88 | 0.00 | -0.04 | -0.37 | 225.24 | 225.24 | 51.96 | 0.262 | 1.088E+07 | 4.741E-03 | 2.956E-03 | 1.784E-03 |
| 6.78 | 11.28 | 0.00 | -0.05 | -0.41 | 225.24 | 225.24 | 51.96 | 0.276 | 1.146E+07 | 4.885E-03 | 2.930E-03 | 1.954E-03 |
| 7.11 | 12.79 | 0.00 | -0.06 | -0.45 | 225.24 | 225.24 | 51.96 | 0.289 | 1.203E+07 | 5.021E-03 | 2.906E-03 | 2.116E-03 |
| 7.45 | 14.38 | 0.00 | -0.06 | -0.50 | 225.24 | 225.24 | 51.96 | 0.303 | 1.260E+07 | 5.144E-03 | 2.883E-03 | 2.261E-03 |
| 7.79 | 16.05 | 0.00 | -0.06 | -0.55 | 225.24 | 225.24 | 51.96 | 0.317 | 1.318E+07 | 5.253E-03 | 2.861E-03 | 2.392E-03 |
| 8.13 | 17.82 | 0.00 | -0.05 | -0.60 | 225.24 | 225.24 | 51.96 | 0.331 | 1.375E+07 | 5.357E-03 | 2.841E-03 | 2.516E-03 |
| 8.47 | 19.94 | 0.00 | -0.02 | -0.67 | 225.24 | 225.24 | 51.96 | 0.344 | 1.432E+07 | 5.524E-03 | 2.821E-03 | 2.703E-03 |
| 8.81 | 22.27 | 0.00 | 0.03 | -0.74 | 225.24 | 225.24 | 51.96 | 0.358 | 1.489E+07 | 5.704E-03 | 2.803E-03 | 2.901E-03 |
| 9.15 | 24.94 | 0.00 | 0.11 | -0.81 | 225.24 | 225.24 | 51.96 | 0.372 | 1.547E+07 | 5.923E-03 | 2.785E-03 | 3.138E-03 |
| 9.49 | 28.51 | 0.00 | 0.21 | -0.88 | 225.24 | 225.24 | 51.96 | 0.386 | 1.604E+07 | 6.297E-03 | 2.768E-03 | 3.529E-03 |
| 9.82 | 33.17 | 0.00 | 0.35 | -0.95 | 225.24 | 225.24 | 51.96 | 0.400 | 1.661E+07 | 6.830E-03 | 2.752E-03 | 4.078E-03 |
| 10.16 | 38.05 | 0.00 | 0.51 | -1.01 | 225.24 | 225.24 | 51.96 | 0.413 | 1.719E+07 | 7.321E-03 | 2.737E-03 | 4.584E-03 |
| 10.50 | 42.47 | 0.00 | 0.71 | -1.07 | 225.24 | 225.24 | 51.96 | 0.427 | 1.776E+07 | 7.653E-03 | 2.722E-03 | 4.931E-03 |
| 10.84 | 47.03 | 0.00 | 0.92 | -1.13 | 225.24 | 225.24 | 51.96 | 0.441 | 1.833E+07 | 7.952E-03 | 2.707E-03 | 5.245E-03 |
| 11.18 | 51.97 | 0.00 | 1.13 | -1.19 | 225.24 | 225.24 | 51.96 | 0.455 | 1.890E+07 | 8.262E-03 | 2.694E-03 | 5.569E-03 |
| 11.52 | 57.29 | 0.00 | 1.34 | -1.25 | 225.24 | 225.24 | 51.96 | 0.469 | 1.948E+07 | 8.581E-03 | 2.681E-03 | 5.900E-03 |

**Table III-2**

**Faired Resistance Data for Bare Hull Model 5482-1**

**Title:** Waterjet Concept
**Model Name:** 5482-1
**Model Weight:** 1212.00 lbs
**Longitudinal C.G, Ref:** From Mid Ship
**Longitudinal C.G:** -13.23 in
**Frontal Area:** 0.00 sqin
**Stimulator:** Studs
**Stimulator Penalty:** 0.000E+00
**Correlation Allowance:** 4.000E-04

**Friction Line:** ITTC
**Working Fluid:** Fresh Water
**Water Temperature:** 66.0°F
**Water Density:** 1.937 sl/ft^3
**Water Viscosity:** 1.110E-05 ft^2/sec
**Air Temperature:** 74.0°F
**Air Density:** 2.311E-03 ft^2/sec
**Air Viscosity:** 1.657E-04 ft^2/sec
**Assumed Aero Drag Coef:** 0.000

**Labotatory:** NSWC
**Code Name:** Seakeeping
**Code Number:** Code 5500
**Experimentors:** Burke, Hickok, Hoyt III
**Facility:** Shallow Basin
**Carriage:** Carriage 1
**Test Period:** January 1997
**Sponsor:** ONR
**Job Order Number:** 1-5060-753-20

| Hull Speed Vm (fps) | Total Resistance Rtm (lbs) | Areo Resistance Ram (lbs) | Running Trim Pm (deg) | Heave Disp Zm (in) | Wetted Length Fn WLfm (in) | Wetted Length Rn WLrm (in) | Wetted Surface WSAm (sqft) | Froude Number Fn | Reynolds Number Rnm | Total Drag Coef Ctm | Friction Coef Cfm | Residual Coef Cr |
|---|---|---|---|---|---|---|---|---|---|---|---|---|
| 2.67 | 1.71 | 0.00 | -0.01 | -0.05 | 225.24 | 225.24 | 51.96 | 0.108 | 4.510E+06 | 4.775E-03 | 3.462E-03 | 1.313E-03 |
| 3.36 | 2.67 | 0.00 | -0.02 | -0.07 | 225.24 | 225.24 | 51.96 | 0.137 | 5.678E+06 | 4.700E-03 | 3.318E-03 | 1.381E-03 |
| 4.03 | 3.76 | 0.00 | -0.02 | -0.12 | 225.24 | 225.24 | 51.96 | 0.164 | 6.820E+06 | 4.591E-03 | 3.210E-03 | 1.381E-03 |
| 4.04 | 4.44 | 0.00 | -0.03 | -0.12 | 225.24 | 225.24 | 51.96 | 0.164 | 6.827E+06 | 5.418E-03 | 3.209E-03 | 2.209E-03 |
| 4.70 | 4.99 | 0.00 | -0.03 | -0.18 | 225.24 | 225.24 | 51.96 | 0.191 | 7.941E+06 | 4.501E-03 | 3.124E-03 | 1.377E-03 |
| 4.70 | 5.21 | 0.00 | -0.03 | -0.16 | 225.24 | 225.24 | 51.96 | 0.191 | 7.956E+06 | 4.676E-03 | 3.123E-03 | 1.553E-03 |
| 5.36 | 7.18 | 0.00 | -0.05 | -0.25 | 225.24 | 225.24 | 51.96 | 0.218 | 9.058E+06 | 4.975E-03 | 3.052E-03 | 1.923E-03 |
| 6.05 | 9.20 | 0.00 | -0.05 | -0.33 | 225.24 | 225.24 | 51.96 | 0.246 | 1.023E+07 | 4.996E-03 | 2.988E-03 | 2.008E-03 |
| 6.72 | 11.82 | 0.00 | -0.06 | -0.41 | 225.24 | 225.24 | 51.96 | 0.273 | 1.137E+07 | 5.196E-03 | 2.934E-03 | 2.262E-03 |
| 6.73 | 12.10 | 0.00 | -0.07 | -0.42 | 225.24 | 225.24 | 51.96 | 0.274 | 1.138E+07 | 5.305E-03 | 2.934E-03 | 2.371E-03 |
| 7.43 | 15.54 | 0.00 | -0.04 | -0.50 | 225.24 | 225.24 | 51.96 | 0.302 | 1.256E+07 | 5.597E-03 | 2.885E-03 | 2.713E-03 |
| 8.08 | 18.04 | 0.00 | -0.05 | -0.62 | 225.24 | 225.24 | 51.96 | 0.329 | 1.366E+07 | 5.493E-03 | 2.844E-03 | 2.649E-03 |
| 8.08 | 17.98 | 0.00 | -0.04 | -0.62 | 225.24 | 225.24 | 51.96 | 0.329 | 1.366E+07 | 5.474E-03 | 2.844E-03 | 2.630E-03 |
| 8.09 | 18.87 | 0.00 | -0.05 | -0.59 | 225.24 | 225.24 | 51.96 | 0.329 | 1.367E+07 | 5.736E-03 | 2.843E-03 | 2.893E-03 |
| 8.76 | 23.69 | 0.00 | -0.01 | -0.68 | 225.24 | 225.24 | 51.96 | 0.356 | 1.482E+07 | 6.130E-03 | 2.805E-03 | 3.325E-03 |
| 9.41 | 29.58 | 0.00 | 0.15 | -0.76 | 225.24 | 225.24 | 51.96 | 0.383 | 1.592E+07 | 6.632E-03 | 2.772E-03 | 3.861E-03 |
| 9.42 | 29.53 | 0.00 | 0.16 | -0.77 | 225.24 | 225.24 | 51.96 | 0.383 | 1.593E+07 | 6.616E-03 | 2.771E-03 | 3.844E-03 |
| 10.10 | 40.63 | 0.00 | 0.49 | -0.77 | 225.24 | 225.24 | 51.96 | 0.411 | 1.708E+07 | 7.915E-03 | 2.739E-03 | 5.176E-03 |
| 10.10 | 40.66 | 0.00 | 0.50 | -0.76 | 225.24 | 225.24 | 51.96 | 0.411 | 1.709E+07 | 7.916E-03 | 2.739E-03 | 5.177E-03 |
| 10.74 | 50.97 | 0.00 | 0.81 | -0.68 | 225.24 | 225.24 | 51.96 | 0.437 | 1.817E+07 | 8.775E-03 | 2.711E-03 | 6.064E-03 |

**Table III-3**

**Raw Resistance Data for Bare Hull Model 5482-1 with 5-Hole Velocity Probe in Place**

| Title: | Waterjet Concept | Friction Line: | ITTC | Labotatory: | NSWC |
|---|---|---|---|---|---|
| Model Name: | 5482-1 | Working Fluid: | Fresh Water | Code Name: | Seakeeping |
| Model Weight: | 1212.00 lbs | Water Temperature: | 66.0°F | Code Number: | Code 5500 |
| Longitudinal C.G, Ref: | From Mid Ship | Water Density: | 1.937 sl/ft^3 | Experimentors: | Burke, Hickok, Hoyt III |
| Longitudinal C.G: | -13.23 in | Water Viscosity: | 1.110E-05 ft^2/sec | Facility: | Shallow Basin |
| Frontal Area: | 0.00 sqin | Air Temperature: | 74.0°F | Carriage: | Carriage 1 |
| Stimulator: | Studs | Air Density: | 2.311E-03 ft^2/sec | Test Period: | January 1997 |
| Stimulator Penalty: | 0.000E+00 | Air Viscosity: | 1.657E-04 ft^2/sec | Sponsor: | ONR |
| Correlation Allowance: | 4.000E-04 | Assumed Aero Drag Coef.: | 0.000 | Job Order Number: | 1-5060-753-20 |

| Hull Speed Vm (fps) | Total Resistance Rtm (lbs) | Areo Resistance Ram (lbs) | Running Trim Pm (deg) | Heave Disp Zm (in) | Wetted Length Fn WLfm (in) | Wetted Length Rn WLrm (in) | Wetted Surface WSAm (sqft) | Froude Number Fn | Reynolds Number Rnm | Total Drag Coef Ctm | Friction Coef Cfm | Residual Coef Cr |
|---|---|---|---|---|---|---|---|---|---|---|---|---|
| 0.00 | 0.00 | 0.00 | 0.00 | 0.00 | 225.24 | 225.24 | 51.96 | 0.000 | 0.000E+00 | | | |
| 0.34 | 0.04 | 0.00 | 0.00 | 0.00 | 225.24 | 225.24 | 51.96 | 0.014 | 5.729E+05 | 7.182E-03 | 5.311E-03 | 1.871E-03 |
| 0.68 | 0.14 | 0.00 | 0.00 | 0.00 | 225.24 | 225.24 | 51.96 | 0.028 | 1.146E+06 | 6.157E-03 | 4.552E-03 | 1.605E-03 |
| 1.02 | 0.29 | 0.00 | -0.01 | -0.01 | 225.24 | 225.24 | 51.96 | 0.041 | 1.719E+06 | 5.657E-03 | 4.181E-03 | 1.475E-03 |
| 1.36 | 0.49 | 0.00 | -0.01 | -0.01 | 225.24 | 225.24 | 51.96 | 0.055 | 2.291E+06 | 5.341E-03 | 3.945E-03 | 1.396E-03 |
| 1.69 | 0.74 | 0.00 | -0.01 | -0.02 | 225.24 | 225.24 | 51.96 | 0.069 | 2.864E+06 | 5.120E-03 | 3.775E-03 | 1.345E-03 |
| 2.03 | 1.03 | 0.00 | -0.01 | -0.03 | 225.24 | 225.24 | 51.96 | 0.083 | 3.437E+06 | 4.959E-03 | 3.645E-03 | 1.315E-03 |
| 2.37 | 1.37 | 0.00 | -0.01 | -0.04 | 225.24 | 225.24 | 51.96 | 0.096 | 4.010E+06 | 4.848E-03 | 3.540E-03 | 1.308E-03 |
| 2.71 | 1.76 | 0.00 | -0.01 | -0.05 | 225.24 | 225.24 | 51.96 | 0.110 | 4.583E+06 | 4.769E-03 | 3.452E-03 | 1.317E-03 |
| 3.05 | 2.20 | 0.00 | -0.02 | -0.06 | 225.24 | 225.24 | 51.96 | 0.124 | 5.156E+06 | 4.712E-03 | 3.378E-03 | 1.335E-03 |
| 3.39 | 2.72 | 0.00 | -0.02 | -0.08 | 225.24 | 225.24 | 51.96 | 0.138 | 5.729E+06 | 4.703E-03 | 3.313E-03 | 1.390E-03 |
| 3.73 | 3.32 | 0.00 | -0.02 | -0.11 | 225.24 | 225.24 | 51.96 | 0.152 | 6.302E+06 | 4.752E-03 | 3.256E-03 | 1.496E-03 |
| 4.07 | 3.99 | 0.00 | -0.02 | -0.13 | 225.24 | 225.24 | 51.96 | 0.165 | 6.874E+06 | 4.795E-03 | 3.205E-03 | 1.590E-03 |
| 4.40 | 4.68 | 0.00 | -0.02 | -0.16 | 225.24 | 225.24 | 51.96 | 0.179 | 7.447E+06 | 4.800E-03 | 3.160E-03 | 1.640E-03 |
| 4.74 | 5.41 | 0.00 | -0.02 | -0.19 | 225.24 | 225.24 | 51.96 | 0.193 | 8.020E+06 | 4.776E-03 | 3.118E-03 | 1.658E-03 |
| 5.08 | 6.18 | 0.00 | -0.03 | -0.23 | 225.24 | 225.24 | 51.96 | 0.207 | 8.593E+06 | 4.759E-03 | 3.081E-03 | 1.678E-03 |
| 5.42 | 7.08 | 0.00 | -0.03 | -0.26 | 225.24 | 225.24 | 51.96 | 0.220 | 9.166E+06 | 4.786E-03 | 3.046E-03 | 1.740E-03 |
| 5.76 | 8.16 | 0.00 | -0.03 | -0.30 | 225.24 | 225.24 | 51.96 | 0.234 | 9.739E+06 | 4.886E-03 | 3.014E-03 | 1.873E-03 |
| 6.10 | 9.39 | 0.00 | -0.04 | -0.33 | 225.24 | 225.24 | 51.96 | 0.248 | 1.031E+07 | 5.018E-03 | 2.984E-03 | 2.034E-03 |
| 6.44 | 10.73 | 0.00 | -0.04 | -0.37 | 225.24 | 225.24 | 51.96 | 0.262 | 1.088E+07 | 5.147E-03 | 2.956E-03 | 2.190E-03 |
| 6.78 | 12.20 | 0.00 | -0.05 | -0.41 | 225.24 | 225.24 | 51.96 | 0.276 | 1.146E+07 | 5.280E-03 | 2.930E-03 | 2.349E-03 |
| 7.11 | 13.77 | 0.00 | -0.06 | -0.45 | 225.24 | 225.24 | 51.96 | 0.289 | 1.203E+07 | 5.407E-03 | 2.906E-03 | 2.502E-03 |
| 7.45 | 15.46 | 0.00 | -0.06 | -0.50 | 225.24 | 225.24 | 51.96 | 0.303 | 1.260E+07 | 5.532E-03 | 2.883E-03 | 2.649E-03 |
| 7.79 | 17.21 | 0.00 | -0.06 | -0.55 | 225.24 | 225.24 | 51.96 | 0.317 | 1.318E+07 | 5.633E-03 | 2.861E-03 | 2.772E-03 |
| 8.13 | 19.17 | 0.00 | -0.05 | -0.60 | 225.24 | 225.24 | 51.96 | 0.331 | 1.375E+07 | 5.762E-03 | 2.841E-03 | 2.922E-03 |
| 8.47 | 21.44 | 0.00 | -0.02 | -0.67 | 225.24 | 225.24 | 51.96 | 0.344 | 1.432E+07 | 5.940E-03 | 2.821E-03 | 3.118E-03 |
| 8.81 | 24.07 | 0.00 | 0.03 | -0.74 | 225.24 | 225.24 | 51.96 | 0.358 | 1.489E+07 | 6.166E-03 | 2.803E-03 | 3.364E-03 |
| 9.15 | 27.08 | 0.00 | 0.11 | -0.81 | 225.24 | 225.24 | 51.96 | 0.372 | 1.547E+07 | 6.431E-03 | 2.785E-03 | 3.646E-03 |
| 9.49 | 31.00 | 0.00 | 0.21 | -0.88 | 225.24 | 225.24 | 51.96 | 0.386 | 1.604E+07 | 6.846E-03 | 2.768E-03 | 4.078E-03 |
| 9.82 | 36.15 | 0.00 | 0.35 | -0.95 | 225.24 | 225.24 | 51.96 | 0.400 | 1.661E+07 | 7.442E-03 | 2.752E-03 | 4.690E-03 |
| 10.16 | 41.58 | 0.00 | 0.51 | -1.01 | 225.24 | 225.24 | 51.96 | 0.413 | 1.719E+07 | 7.999E-03 | 2.737E-03 | 5.263E-03 |
| 10.50 | 47.07 | 0.00 | 0.71 | -1.07 | 225.24 | 225.24 | 51.96 | 0.427 | 1.776E+07 | 8.481E-03 | 2.722E-03 | 5.760E-03 |
| 10.84 | 52.62 | 0.00 | 0.92 | -1.13 | 225.24 | 225.24 | 51.96 | 0.441 | 1.833E+07 | 8.898E-03 | 2.707E-03 | 6.191E-03 |
| 11.18 | 58.56 | 0.00 | 1.13 | -1.19 | 225.24 | 225.24 | 51.96 | 0.455 | 1.890E+07 | 9.311E-03 | 2.694E-03 | 6.617E-03 |
| 11.52 | 64.93 | 0.00 | 1.34 | -1.25 | 225.24 | 225.24 | 51.96 | 0.469 | 1.948E+07 | 9.724E-03 | 2.681E-03 | 7.044E-03 |

**Table III-4**

**Faired Resistance Data for Bare Hull Model 5482-1 with 5-Hole Velocity Probe in Place**